BI-PERSPECTIVE SPLITTING DEFENSE: ACHIEVING CLEAN-DATA-FREE BACKDOOR SECURITY

Anonymous authors
Paper under double-blind review

ABSTRACT

Backdoor attacks have seriously threatened deep neural networks (DNNs) by embedding concealed vulnerabilities through data poisoning. To counteract these attacks, training benign models from poisoned data garnered considerable interest from researchers. High-performing defenses often rely on additional clean subsets, which is untenable due to increasing privacy concerns and data scarcity. In the absence of clean subsets, defenders resort to complex feature extraction and analysis, resulting in excessive overhead and compromised performance. In the face of these challenges, we identify the key lies in sufficient utilization of the easier-to-obtain target labels and excavation of clean hard samples. In this work, we propose a Bi-perspective Splitting Defense (BSD). BSD splits the dataset using both semantic and loss statistics characteristics through open set recognition-based splitting (OSS) and altruistic model-based data splitting (ALS) respectively, achieving good clean pool initialization. BSD further introduces class completion and selective dropping strategies in the subsequent pool updates to avoid potential class underfitting and backdoor overfitting caused by loss-guided split. Through extensive experiments on 3 benchmark datasets and against 7 representative attacks, we empirically demonstrate that our BSD is robust across various attack settings. Specifically, BSD has an average improvement in Defense Effectiveness Rating (DER) by 16.29% compared to 5 state-of-the-art defenses, achieving clean-data-free backdoor security with minimal compromise in both Clean Accuracy (CA) and Attack Success Rate (ASR).

1 INTRODUCTION

Recent studies exposed the vulnerabilities of deep neural networks (DNNs) to various attacks (Carlini & Wagner, 2017; Moosavi-Dezfooli et al., 2016; Kurakin et al., 2018; Zeng et al., 2019; Ilyas et al., 2018), among which backdoor attacks (Li et al., 2022; Wenger et al., 2021; Zhang et al., 2021; Wang et al., 2020) have emerged as a significant threat due to their ease of execution and profound impact. Owing to their non-model-manipulation property and congruence with actual model training scenarios, data-poisoning-based backdoor attacks (Goldblum et al., 2022; Shafahi et al., 2018) stand out as prevalent and impactful threats, highlighting the importance of backdoor defense research. Taking facial recognition as an example (Figure 1), poisoned data may induce the DNNs to erroneously learn a strong correlation between the adversary-defined trigger pattern (e.g., sunglasses) and the target label (e.g., a high-authority individual). While behaving normally without the trigger, the backdoored model predicts any individuals wearing sunglasses as the pre-determined high-authority person. Following the current mainstream research on backdoor attacks, we focus on image classification tasks as the entry point for studying backdoor defenses.

Recently, a branch of in-training defenses has focused on training benign models directly from poisoned data, which is particularly significant when developing our own models using untrustworthy datasets. They primarily adhere to a data-splitting paradigm that differentiates between benign and poisoned samples, and disrupts the association between trigger patterns and target labels to mitigate backdoor behaviors. To name a few, Anti-backdoor learning (ABL) (Li et al., 2021a) isolates poisoned samples through local gradient ascent and unlearns the underlying malicious pattern. Decoupling-based defense (DBD) (Huang et al., 2022) utilizes self-supervised learning for a secure feature extractor to identify unconfident samples as malicious. Adaptive splitting-based defense (ASD) (Gao et al., 2023) further introduces meta-split to identify clean hard samples.

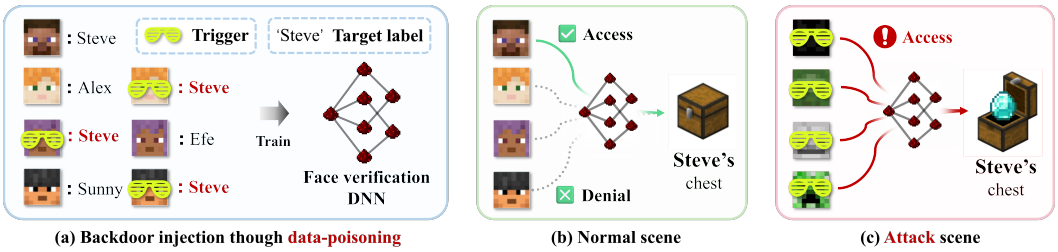

(a) Backdoor injection though data-poisoning (b) Normal scene (c) Attack scene

Figure 1: Illustration of data-poisoning-based backdoor attacks.

Intuitively, clean subsets play a vital role in various backdoor defenses (Zhu et al., 2024; Liu et al., 2018; Wu & Wang, 2021; Zeng et al., 2021; Li et al., 2023a), as they could provide insight into the decision-making features of clean samples (e.g., as long as we know the facial characteristics of people, we can accurately recognize them without being misled by accessories). In-training defenses rely on clean seed samples for better performance (Gao et al., 2023). However, recollecting a clean subset can be extremely expensive when the training set has a large number of classes (e.g., collecting new benign facial records for millions of people within the facial database), and manually checking a large training set to select a clean subset is time-consuming and risky for privacy leaks. In addition, the potential presence of stealthy malicious 'clean sets' can further undermine the effectiveness of these defenses, as triggers like sunglasses and image warping are hard to identify. While certain in-training defenses seek to work without clean subsets, they may involve complicated feature extraction and analysis, suffering from significant training costs (Huang et al., 2022) and compromised performance (Li et al., 2021a; Chen et al., 2022a; Tran et al., 2018; Weber et al., 2023; Liu et al., 2023).

In this work, we focus on improving the state-of-the-art in-training defense under the challenging non-clean-seed-involved scenario. We identify the insufficient utilization of the easier-to-obtain target labels and clean hard samples of existing methods, and propose a Bi-perspective Splitting Defense (BSD) that splits the dataset using both semantic and loss statistics characteristics of poisoned samples.

Specifically, BSD first initialize the clean and poison pools through open set recognition-based splitting (OSS) and altruistic model-based data splitting (ALS). OSS reframes the identification of poisoned samples within the target class as an open-set recognition problem. Non-target classes are designated as known-known classes (KKCs) to warm up the main model, thus true clean samples within the target class are distinguished as an unknown-unknown class (UUC) because their semantic information is unseen to the model. ALS utilizes an altruistic model to reveal reliable clean hard samples with high loss difference to the main model. Since the above two mechanisms complement each other by employing different judgment perspectives, the intersection of their results provides a robust initialization.

Subsequently, to prevent potential underfitting of certain classes (i.e., clean pools do not encompass all the classes) and to capture evasive poisoned samples (i.e., clean pools include some poisoned samples), BSD adopts class completion and selective dropping strategies during subsequent pool updates, ameliorating the loss-perspective-only splitting result.

In summary, our main contributions are:

- We investigate the realistic and challenging task of training time backdoor defense without clean seed samples, and identify two main breakthrough points of the problem.
- We propose two novel pool initialization mechanisms in BSD, namely ALS and OSS. They leverage the loss statistics of clean hard samples based on altruistic models and reframe the splitting as an open set recognition task for better initialization respectively, accomplishing effective backdoor defense free from the clean seed samples.
- We introduce two new pool update strategies based on the altruistic model to address the potential collapse. Class completion and selective dropping deal with the missing classes and evaded poison samples respectively.
- Extensive experiments demonstrate that BSD has an average improvement in Defense Effectiveness Rating (DER) by 16.29% compared to 5 state-of-the-art defenses.

2 RELATED WORKS

Currently, the countermeasures for backdoor attacks fall into two main categories:

Post-training backdoor defenses focus on repairing a backdoored model with a set of locally prepared clean training sets. Trigger inversion (Sur et al., 2023) is a popular method to reconstruct the trigger pattern and then unlearn it to renovate the model. In addition to trigger-synthesis defenses, pruning, distillation, finetuning, and model connectivity analysis (Liu et al., 2018; Wu & Wang, 2021; Li et al., 2023a) are widely applied in the realm of backdoor defense as well. Despite the promising results, most post-training methods assume using an extra clean set for defense, which introduces potential limitations.

In-training backdoor defenses aim at training a benign model from the polluted dataset, which holds considerable practical significance (Chen et al., 2022a; Tran et al., 2018; Weber et al., 2023; Liu et al., 2023). Following an intuitive idea of splitting the dataset into clean and poison pools and treating them separately, several representative training-time defenses, namely Anti-backdoor learning (ABL) (Li et al., 2021a), Decoupled-based defense (DBD) (Huang et al., 2022), and Adaptive splitting-based defense (ASD) (Gao et al., 2023), have garnered attention. Anti-backdoor learning (ABL) (Li et al., 2021a) isolates a small ratio of poisoned samples through local gradient ascent and unlearns these samples to neutralize the effect of remaining poisoned samples in the clean pool. Decoupling-based defense (DBD) (Huang et al., 2022) utilizes self-supervised learning to acquire a benign feature extractor and uses a clean subset to initialize the classifier head. Then, it separates the suspicious according to the loss magnitude and breaks the link between the trigger and the target label through semi-supervised learning. Adaptive splitting-based defense (ASD) (Gao et al., 2023) further improves the initialization based on clean seed samples and introduces meta-split to identify clean hard samples, achieving higher clean accuracy (CA). Besides these defenses, adopting differential-privacy SGD (Du et al., 2019) and strong data augmentation (Borgnia et al., 2021) can also defend against backdoor attacks to some degree. Our BSD belongs to the data-splitting in-training defenses and makes further adaptions.

3 PRELIMINARIES

3.1 THREAT MODEL

Following Gao et al. (2023), We adopt the poisoning-based threat model used in previous works (Gu et al., 2017; Chen et al., 2017; Turner et al., 2018), where the training dataset contains a set of pre-crafted poisoned samples provided by attackers. As a typical setting of training-time defenses in previous works (Gao et al., 2023; Borgnia et al., 2021; Du et al., 2019; Huang et al., 2022; Li et al., 2021a), we assume that defenders have control over the training process.

3.2 PROBLEM FORMULATION

The malicious training set from the adversaries can be denoted as $\mathcal{D} = \mathcal{D}_c \cup \mathcal{D}_p$, where $\mathcal{D}_c$ is a subset of the raw benign dataset $\mathcal{D}_{\text{raw}} = \{(x_i, y_i)\}_{i=1}^{N}$. Each $x_i \in \mathcal{X} \subset \mathbb{R}^{C\times W\times H}$. The ground-truth labels $y_i \in \mathcal{Y} = \{0, 1, \ldots, C-1\}$, with C being the number of categories. Given the poisoning rate ρ, $\mathcal{D}_c$ has $(1-\rho)N$ samples. The poisoned set $\mathcal{D}_p = \{(G(x), T(y)) \mid (x, y) \in \mathcal{D}_{raw} \backslash \mathcal{D}_c\}$, where $G : \mathcal{X} \to \mathcal{X}, T : \mathcal{Y} \to \mathcal{Y}$ are the attack-specific poisoned image generator and label modifier. As an example, $G(x) = m \odot x + (1-m) \odot t, T(x) = y_t$, where the mask $m \in \{0, 1\}^{C\times W\times H}, t \in \mathcal{X}$ is the trigger pattern, and y_t is the target label. We call the $\{(x, y)|y \neq y_t, (x, y) \in \mathcal{D}\}$ as non-target samples $\mathcal{D}_{\text{nt}}$, and $\{(x, y)|y = y_t, (x, y) \in \mathcal{D}\}$ as target samples $\mathcal{D}_{\text{t}}$, $\{(x, y)|y = y_t, (x, y) \in \mathcal{D}_b\}$ as clean target samples $\mathcal{D}_{\text{ct}}$.

Following the natural idea to exclude the poison samples from the training set, defenders can divide $\mathcal{D}$ into a clean pool $\mathcal{D}_{\tilde{c}}$ and a poison pool $\mathcal{D}_{\tilde{p}}$. To prevent the model from being backdoored while preserving the performance on benign samples, the core is breaking the link between triggers and target labels, and making the best of the poison pool. We follow DBD and ASD to use semi-supervised learning (Berthelot et al., 2019b) that only leverages visual features of samples in the poison pool:

$$\mathcal{L}_{\text{semi}} = \sum_{(x,y)\in\mathcal{D}_{\tilde{c}}} \mathcal{L}_s\left(x, y; \theta\right) + \lambda \sum_{x\in\mathcal{D}_{\tilde{c}}\backslash\mathcal{D}_{\tilde{p}}} \mathcal{L}_u\left(x; \theta\right), \tag{1}$$

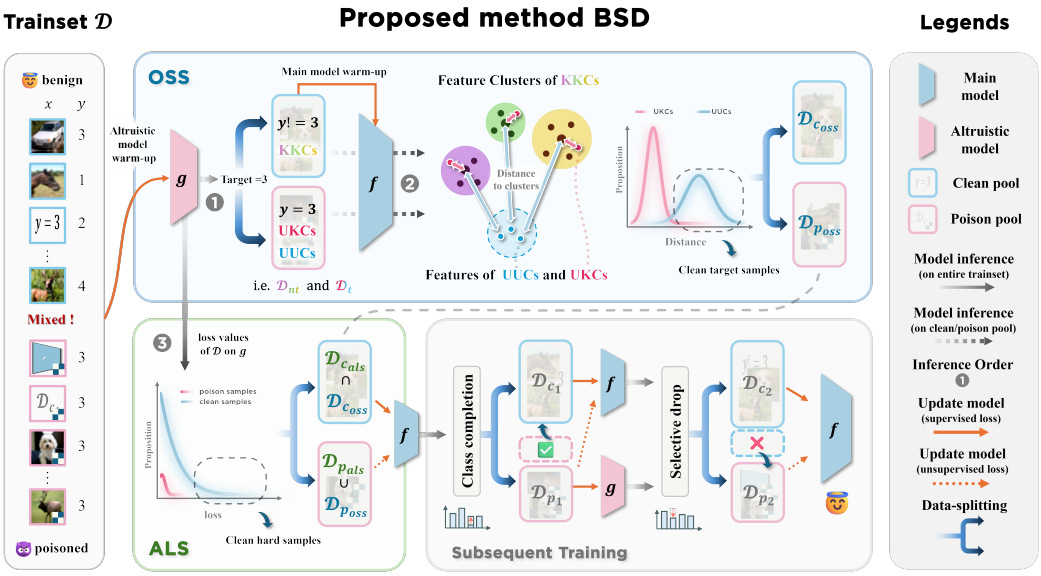

Figure 2: An overview of our BSD. BSD consists of two main initialize mechanisms, i.e., open set recognition-based splitting (OSS) and altruistic model-based splitting (ALS). BSD use the intersection of $\mathcal{D}_{c_{oss}}$ and $\mathcal{D}_{c_{als}}$ from OSS and ALS as the clean pool initialization. In the next two stages of the subsequent training, BSD dynamically updates the clean and poison pools based on a loss-guided split strategy based on the loss discrepancy of the main model f_θ and the altruistic model g_φ. The pseudo-code of BSD is provided in Appendix B.

where θ denote the weights of the main model $f(x;\theta)$ (f_θ for simplicity), $\mathcal{L}_s$ is a common supervised loss function such as cross-entropy loss, the unsupervised $\mathcal{L}_u$ is applied on the suspicious polluted set $\mathcal{D}_{\tilde{c}} \backslash \mathcal{D}_{\tilde{p}}$, with a trade-off coefficient λ. Appendix C.6 provides a detailed definition of semi-supervised learning.

The main task under this framework lies in finding an appropriate indicator that helps maximize the difference between benign and poisoned samples, thus returning a clean pool with high precision and a poison pool with high recall, i.e.:

$$\min_{\mathcal{D}_{\tilde{c}}} |\mathcal{D}_p \cap \mathcal{D}_{\tilde{c}}| \text{ s.t. } \mathcal{D}_{\tilde{c}} \subset \mathcal{D}, \ \max_{\mathcal{D}_{\tilde{p}}} |\mathcal{D}_p \cap \mathcal{D}_{\tilde{p}}| \text{ s.t. } \mathcal{D}_{\tilde{p}} \subset \mathcal{D}. \tag{2}$$

4 Proposed Method

Our BSD has three main components as illustrated in Figure 2. As we assume no extra clean subset access, pool initialization is vital to the defense. To ensure a secure initialization, open set recognition-based splitting (OSS) and altruistic model-based splitting (ALS) focus on the perspectives of image **semantic information** and **loss statistics** respectively. Based on the altruistic model introduced in ALS, we further improve the pool update with class completion and selective dropping strategy.

(1) OSS is motivated by the similarity between the open-set recognition task and poison sample detection in backdoor defense. As the main model is warmed up using $\mathcal{D}_{\text{nt}}$, poison samples are unknown-known-classes (UKCs) whose semantic information is included in $\mathcal{D}_{\text{nt}}$, thus having smaller minimum distances to feature clusters of known-known-classes (KKCs). Clean target samples fall into a new cluster and have larger minimum distances. Detailed description in Section 4.1.1.

(2) ALS highlights the clean hard samples with high loss values in the altruistic model, which could filter out the overfitted poison samples. A detailed description of ALS is provided in Section 4.1.2.

(3) Subsequent training of BSD follow a loss-guided split, which uses the loss difference of a sample between the main and altruistic model to distinguish samples. BSD compensates the less selected categories and drops the evaded poison samples using class completion and selective dropping strategies respectively. A detailed description of subsequent training is provided in Section 4.2.

4.1 THE INITIALIZATION OF CLEAN AND POISON POOLS

The initialization of the clean and poison pool is then obtained by intersecting the consensual clean samples in ALS and OSS:

$$\mathcal{D}_{\tilde{c}} = \mathcal{D}_{c_{als}} \cap \mathcal{D}_{c_{oss}},\ \mathcal{D}_{\tilde{p}} = \mathcal{D}_{p_{als}} \cup \mathcal{D}_{p_{oss}}, \tag{3}$$

where the $\mathcal{D}_{c_{als}}$ and $\mathcal{D}_{p_{als}}$ is the split result of ALS, $\mathcal{D}_{c_{oss}}$ and $\mathcal{D}_{p_{oss}}$ is the split result of OSS. The following two subsections will explain the two initialization mechanisms.

4.1.1 OPENSET RECOGNITION BASED SPLITING

Openset recognition (OSR) is a task that aims to identify whether a test sample belongs to one of the semantic classes in a classifier's training set. In the context of OSR, identifying unknown-known classes (UKCs) and unknown-unknown classes (UUCs) are two major tasks. Here UKCs refer to classes for which no samples are available in training, but their side information (such as semantic/attribute information, etc.) can be obtained during training. UUCs refer to classes that do not have any relevant information during the training process: not only have they not been seen, but there is also no side information during the training process.

We notice that distinguishing the clean target samples and poison samples is related to the UKCs and UUCs identification in OSR. The poison samples are sort of UKCs because the triggers do not corrupt their semantic information. Hence, we set out to cast the clean target samples to UUCs, which can reframe the splitting within the target class into an OSR problem.

To make the poison samples and clean target samples belong to the UKCs and UUCs respectively, the known-known classes (KKCs, i.e. the training set) should contain the semantic classes of UKCs ($\mathcal{D}_p$), while information of the UUCs ($\mathcal{D}_{\mathrm{ct}}$) is not included. Therefore, we construct the KKCs with the non-target classes ($\mathcal{D}_{\mathrm{nt}}$) which satisfies both requirements above. Thus, we can train the main model f_θ on $\mathcal{D}_{\mathrm{nt}}$ for its warm-up, i.e., $\theta = \mathrm{argmin}\mathcal{L}_{\mathrm{semi}}(\mathcal{D}_{\mathrm{nt}}; f_\theta)$.

Now the local detection of poisoned samples in $\mathcal{D}_{\mathrm{t}}$ has been reframed as an open set recognition problem. The clean pool identified by OSS can be acquired by adding the approximated UUCs ($\mathcal{D}_{\tilde{\mathrm{ct}}}$) to the KKCs ($\mathcal{D}_{\mathrm{nt}} = \{(x, y) | y \neq y_t, (x, y) \in \mathcal{D}\}$):

$$\mathcal{D}_{c_{\mathrm{oss}}} = \mathcal{D}_{\tilde{\mathrm{ct}}} \cup \mathcal{D}_{\mathrm{nt}},\ \mathcal{D}_{p_{\mathrm{oss}}} = \mathcal{D} \backslash \mathcal{D}_{c_{\mathrm{oss}}}. \tag{4}$$

To approximate the $\mathcal{D}_{\tilde{\mathrm{ct}}}$ in the reframed problem, it's ideal to have the known-unknown classes (KUCs), which again indicates the need for clean seed samples. Fortunately, there have been a lot of previous studies on solving this problem without KUCs. We approximate $\mathcal{D}_{\tilde{\mathrm{ct}}}$ by:

$$\mathcal{D}_{\tilde{\mathrm{ct}}} = \left\{(x, y) \mid \mathcal{S}(x) \geq \mathrm{Percentile}\left(\mathcal{D}_{\mathrm{t}}^{\mathcal{S}}, 1 - \beta\right)\right\}, \tag{5}$$

where β is a fixed ratio of samples in $\mathcal{D}_{\mathrm{t}}$ to be added to $\mathcal{D}_{\mathrm{nt}}$, $\mathcal{D}_t^{\mathcal{S}} = \{\mathcal{S}(x) \mid (x, y) \in \mathcal{D}_t\}$ is the mapped $\mathcal{D}$ using $\mathcal{S}$. Motivated by OpenMAX (Bendale & Boult, 2016), we take the feature distance to KKCs as a metric to measure the likelihood of a sample within $\mathcal{D}_{\mathrm{t}}$ to be a true clean sample:

$$\mathcal{S}(x) = \min_{i=\{0,1,\ldots,C-1\} \backslash \tilde{y_t}} \{||f_e(x) - \mu_i||_2\}, \tag{6}$$

where f_e is the feature extractor of f, $\mu_i = \frac{1}{N_i} \sum f_e(x_i)$ it the cluster center of each KKC.

Approximating y_t. It should be noted that it requires y_t to construct $\mathcal{D}_{\mathrm{t}}$ and $\mathcal{D}_{\mathrm{nt}}$. Although the target label y_t used in the above process is unknown to the defender, it's easy to approximate. There exist various alternative methods to detect the y_t (Gao et al., 2024; Zhu et al., 2024), we here adopt a lightweight solution by just slightly modifying the warm-up of the altruistic model. We add local gradient ascent (Li et al., 2021a) and a local voting process: $\tilde{y_t} = \arg\max_c |\{(x, y) \mid y = c \wedge (x, y) \in \mathcal{D}_{lga}\}|$, where $\mathcal{D}_{lga}$ denotes the isolated 1% samples having the smallest loss values after local gradient ascent training on the altruistic model. In common scenarios where the dataset is a large but well-known benchmark dataset, the number of samples in each class is known to the public, y_t can be just approximated through label statistics. Appendix B provides a detailed description of this process.

4.1.2 ALTRUISTIC MODEL BASED SPLITTING

In our BSD, we introduce an altruistic model $g(x;\varphi)$ (g_φ for simplicity), which is an independent model having the same structure as the main model. It serves as a pathfinder of the main model by exposing itself to the entire malicious training set, i.e., $\varphi = \mathrm{argmin}\mathcal{L}_{\mathrm{ce}}(\mathcal{D}, g_\varphi)$, where $\mathcal{L}_{\mathrm{ce}}$ stands for the cross-entropy loss.

We calculate the rest unsolved part in equation 3, i.e., $\mathcal{D}_{c_{als}}$ and $\mathcal{D}_{p_{als}}$ following the equation below:

$$\mathcal{D}_{c_{als}} = \left\{(x,y) \,|\, \mathcal{L}(x,y,\varphi) \geq \mathrm{Percentile}\left(\mathcal{D}^{\mathcal{L}}, 1-\alpha\right)\right\},\ \mathcal{D}_{p_{als}} = \mathcal{D} \backslash \mathcal{D}_{c_{als}}, \tag{7}$$

where $\mathcal{L}$ is the symmetric cross-entropy loss (Wang et al., 2019), $\mathcal{D}^{\mathcal{L}} = \{\mathcal{L}(x,y,\varphi) \mid (x,y) \in \mathcal{D}\}$ is loss values using g_φ of the training set, $\mathrm{Percentile}$ returns the α-percentile in $\mathcal{D}^{\mathcal{L}}$, α is the ratio of samples split to the clean pool.

Note that although here the altruistic model is just used for the pool initialization, it also plays a significant role in the subsequent training.

4.2 SUBSEQUENT TRAINING

BSD trains f_θ on two pools according to equation 1 in the subsequent training. Based on the altruistic model g_φ introduced in ALS, BSD adaptively updates the pools according to the loss discrepany of f_θ and g_φ. Two strategies are adopted in BSD to avoid incomplete or poisoned clean pools.

4.2.1 CLASS COMPLETION STRATEGY

Despite securing good pool initialization without involving the clean seed samples, the clean pools may have an unbalanced distribution of classes, hampering the model's performance on clean accuracy. This primarily stems from the imbalanced learning status of categories and the cyclic positive feedback effect of loss-guided methods. We further revise the splitting strategy of clean samples, adding samples in the class with the fewest samples:

$$\begin{aligned}&\mathcal{D}_{\tilde{c_1}} = \left\{(x,y) \,|\, \mathcal{I}(x,y) \geq \mathrm{Percentile}\left(\mathcal{D}^{\mathcal{I}}, 1-\alpha\right) \vee \left\{y=i, \mathcal{I}(x,y) \geq \mathrm{Percentile}\left(\mathcal{D}_i^{\mathcal{I}}, 1-n_i'/N_i\right)\right\}\right\},\\ &\mathcal{D}_{\tilde{p_1}} = \mathcal{D} \backslash \mathcal{D}_{\tilde{c_1}},\end{aligned} \tag{8}$$

where $\mathcal{I}(x,y)$ is an loss based indicator, $\mathcal{D}^{\mathcal{I}} = \{\mathcal{I}(x,y) \mid (x,y) \in \mathcal{D}\}$ is the mapped $\mathcal{D}$ using $\mathcal{I}$. $\mathcal{D}_i^{\mathcal{I}} = \{\mathcal{I}(x,y) \mid y = i\,(x,y) \in \mathcal{D}\}$, $N_i = |\mathcal{D}_i^{\mathcal{I}}|$, $n_i' = \min\{\alpha n_i, N_{secondFew}\}$, $N_{secondFew}$ is number of samples in the second-fewest predicted class.

We do subtraction between the loss of samples on the main and altruistic models, as the poison samples should also have high loss values on the unaffected main model and low loss values on the backdoored altruistic model. Thus $\mathcal{I}$ is defined as:

$$\mathcal{I}(x,y) = \mathcal{L}_{sce}(x,y,\varphi) - \mathcal{L}_{sce}(x,y,\theta), \tag{9}$$

where $\mathcal{L}_{sce}$ denotes the symmetric cross-entropy loss (Wang et al., 2019).

4.2.2 SELECTIVE DROPPING STRATEGY

Approaching the end of the training, we drop the samples that are predicted to be $\tilde{y_t}$ by both models:

$$\mathcal{D}_{\tilde{c_2}} = \mathcal{D}_{\tilde{c_1}} \setminus \{(x,y) \mid (f(x) = \tilde{y_t}) \wedge (g(x) = \tilde{y_t})\},\ \mathcal{D}_{\tilde{p_2}} = \mathcal{D} \backslash \mathcal{D}_{\tilde{c_2}}, \tag{10}$$

There exist two probable situations for a sample that will be dropped: 1) the sample is poisoned; 2) the sample is a clean sample with the original label being $\tilde{y_t}$. For situation 1, it is the correct decision to drop poisoned samples; for situation 2, the agreement between the two models indicates the sample is already well-fitted by both models and is less important. As a result, the dropping of these samples generally helps improve model performance.

5 EXPERIMENTS

5.1 EXPERIMENTAL SETTINGS

Datasets and DNN models. We adopt three benchmark datasets for the evaluation of the backdoor defenses, namely, CIFAR-10 (Krizhevsky et al., 2009), GTSRB (Stallkamp et al., 2012), and Imagenet (Deng et al., 2009). The results are conducted with ResNet-18 (He et al., 2016) and MobileNet-v2 (Sandler et al., 2018) as the backbone models for their representativeness and widespread use.

Attack Baselines. We implement seven representative attacks, i.e., BadNets (Gu et al., 2017), Blended (Chen et al., 2017), WaNet (Nguyen & Tran, 2021), Label-Consistent(LC) (Turner et al., 2019), ReFool (Liu et al., 2020), SIG (Barni et al., 2019), and Narcissus (Zeng et al., 2023b). All these attacks are implemented based on open-source codebases of ASD (Gao et al., 2023), DBD (Huang et al., 2022), Narcissus (Zeng et al., 2023b), backdoorBench (Wu et al., 2022), and BackdoorBox (Li et al., 2023b). The first five attacks follow the same setting in settings in (Gao et al., 2023) unless otherwise specified, SIG and Narcissus follow the setting with Li et al. (2021a) and Zeng et al. (2023b) respectively, while the poisoning rate ρ and target label y_t are the same as LC. A detailed description of the attack implementations is provided in Appendix C.3.

Defense Baselines. We compare our proposed BSD with five existing backdoor defenses, namely Fine-pruning (FP) (Liu et al., 2018), Neural Attention Distillation (NAD) (Li et al., 2021b), Anti-Backdoor-Learning (ABL) (Li et al., 2021a), Decoupling-based Backdoor Defense (DBD) (Huang et al., 2022), and Adaptive Splitting-based backdoor Defense (ASD) (Gao et al., 2023). The detailed settings for all defense baselines are as suggested in ASD. For our BSD, we adopt the MixMatch (Berthelot et al., 2019b) semi-supervised training framework for the main model, following Decoupling-based Defense (DBD) and Adaptive Splitting-based Defense (ASD). The altruistic model undergoes a warm-up phase with 25 epochs, utilizing the Adam optimizer, cross entropy loss, with a learning rate of 0.001. The default warm-up epochs for the main model in OSS are set to 20 ($T_1 = 20$), with a default fixed β of 0.2. Class completion training spans 60 epochs ($T_2 = 90$), and selective dropping training spans 30 epochs ($T_3 = 120$). The clean pool ratio α follows a sinusoidal growth curve during class rebalance training, starts at 0.2, and reaches an upper limit of 0.6 at the end of the class completion stage, after which it remains fixed. Additional details are available in Appendix C.4.

Evaluation metrics. We assess the effectiveness of backdoor defenses using two widely used metrics: Clean Accuracy (CA) and the attack success rate (ASR). To be specific, the CA is the accuracy of clean data, the ASR is defined as the proportion of poisoned samples that are misclassified as the target class by the model. In the context of backdoor defense, superior performance is characterized by higher CA and lower ASR. To comprehensively evaluate the performance of defense methods, we include another metric named Defense Effectiveness Rating (DER) (Zhu et al., 2023a), higher DER indicate better defense performance. The detailed definition of DER is provided in Appendix C.5.

5.2 MAIN RESULTS

We present a summary of CAs, ASRs, and DERs achieved by five backdoor defenses against three most representative backdoor attacks on three benchmark datasets in Table 1[1]. As illustrated in Table 1, our BSD has the best average DERs on each dataset, being capable of maintaining high CAs without compromising the robustness indicated by ASRs. In comparison with post-training defenses, i.e., FP and NAD, which require thousands of clean seed samples, BSD consistently outperforms them with lower ASRs when OSS is used as the alternative initialization. Additionally, the CAs of BSD surpass those of FP and NAD. Concerning recently proposed training-time defenses, the BSD has best result in general. ABL, which assumes no presence of clean subsets, has relatively close performance under CIFAR-10 & BadNets, GTSRB & BadNets, and GTSRB & Blend. Nevertheless, the CA under CIFAR-10 & WaNet indicates a class underfitting collapse (CAs on certain classes are close to 0%) and its performance is inferior to that of BSD in general. For another representative training-time defense DBD, although it has a slight edge in ASRs on CIFAR-10, its average ASRs and CAs fall behind our BSD. ASD, which assumes an extra small clean seed set is characterized by

[1]Since we strictly follow the same settings, we reference the baseline results for CIFAR-10 and GTSRB from ASD (Gao et al., 2023). However, the exact 30 randomly selected classes from the Imagenet subset used are unknown to us, so we ran all the baselines on Imagenet using our own randomly chosen 30 classes.

Table 1: The clean accuracy (CA%), attack success rate (ASR%), and defense effective rating (DER%) of 5 baseline backdoor defense methods and our BSD against 3 representative backdoor attacks on 3 benchmark datasets. The baselines consist of two post-training defenses (FP, NAD) and three state-of-the-art training-time defenses (ABL, DBD, ASD). 'Non' stands for no defense. The best and second best results are in **bold** and underlined.

Dataset	Attack	Metric	Non	FP	NAD	ABL	DBD	ASD	BSD(ours)
CIFAR-10	BadNet	CA	94.9	93.9	88.2	93.8	92.3	93.4	**95.1**
		ASR	100.0	1.8	4.6	1.1	**0.8**	1.2	0.9
		DER	-	98.6	94.4	**98.9**	98.3	98.7	**99.6**
	Blended	CA	94.1	92.9	85.8	91.9	91.7	93.7	**94.9**
		ASR	98.3	77.1	3.4	1.6	**0.7**	1.6	0.8
		DER	-	60.0	93.3	97.3	97.6	98.2	**98.8**
	WaNet	CA	93.6	90.4	71.3	84.1	91.4	93.1	**94.5**
		ASR	99.9	98.6	6.7	2.2	**0.0**	1.7	0.8
		DER	-	49.1	85.5	94.1	98.9	98.9	**99.6**
	Average DER		-	69.2	91.0	96.8	98.3	98.6	**99.3**
GTSRB	BadNet	CA	97.6	84.2	97.1	97.1	91.4	96.7	**97.6**
		ASR	100.0	**0.0**	0.2	**0.0**	**0.0**	**0.0**	**0.0**
		DER	-	93.3	99.7	99.8	96.9	99.6	**100.0**
	Blended	CA	97.2	91.4	93.3	**97.1**	91.5	**97.1**	96.9
		ASR	99.4	68.1	62.4	0.5	99.9	0.3	**0.0**
		DER	-	62.8	66.6	99.4	46.9	99.5	**99.6**
	WaNet	CA	97.2	92.5	96.5	97.0	89.6	**97.2**	**97.2**
		ASR	100.0	21.4	47.1	0.4	**0.0**	0.3	0.2
		DER	-	87.0	76.1	99.7	96.2	**99.9**	**99.9**
	Average DER		-	81.0	80.8	99.6	80.0	99.6	**99.8**
IMAGENET	BadNet	CA	75.7	71.4	51.7	68.1	76.1	**81.1**	78.3
		ASR	99.5	2.6	2.5	7.6	1.2	100.0	**1.1**
		DER	-	96.3	86.5	92.2	**99.2**	50.0	**99.2**
	Blended	CA	74.5	73.1	42.8	61.9	77.9	79.7	**80.1**
		ASR	97.7	81.9	**0.2**	100.0	35.0	51.0	**0.2**
		DER	-	57.2	82.9	42.6	81.4	73.4	**98.8**
	WaNet	CA	77.1	76.9	74.0	74.9	77.2	78.4	**78.7**
		ASR	81.0	0.4	1.3	1.1	5.2	14.0	**0.0**
		DER	-	90.2	88.3	88.9	87.9	83.5	**90.5**
	Average DER		-	81.2	85.9	74.5	89.5	69.0	**96.2**

consistent high CAs and stable ASRs. However, BSD still surpasses it in general. In summary, our BSD performance remains competitive and, in some cases, surpasses that of state-of-the-art methods.

5.3 Resistance to more attacks

In addition to the representative attacks presented in the main results, we investigated four more attacks that may be threatening to existing defenses. They consist of one invisible attack, ReFool (Liu et al., 2020), and three clean-label attacks, LC (Turner et al., 2019), SIG (Barni et al., 2019), and Narcissus (Zeng et al., 2023b). ReFool uses a physical yet stealthy reflection trigger, which makes the backdoor hard to detect. LC, SIG, and Narcissus belong to the clean-label attack, which is a type of tricky backdoor attack that does not change the label of samples, making most of the defenses ineffective (where DBD has the most significant performance degradation). For our BSD, clean-label attacks are less threatening. While the OSS mechanism can be evaded as the semantic information is $\mathcal{D}_{\mathrm{t}}$ is consistent. Fortunately, ALS still functions effectively with its loss-perspective splitting in this scenario, compensating for the limitations of OSS. As shown in Table 2, BSD is not evaded by any of the attacks and achieves the best average DER. Additional details of attack implementation are available in Appendix C.3.

5.4 Robustness to different model structures

BSD makes no assumptions about model structures, ensuring both compatibility and versatility. To validate this, we evaluated the defense performance of BSD using another widely adopted network, MobileNet (Sandler et al., 2018). As shown in Table 3, BSD consistently outperforms the baseline method with MobileNet-v2 as the backbone.

Table 2: The clean accuracy (CA%), attack success rate (ASR%), and defense effective rating (DER%) of 5 baseline backdoor defense methods and our BSD against 4 threatening backdoor attacks on CIFAR-10. The best and second best results are in **bold** and underlined.

Attack	Metric	Non	FP	NAD	ABL	DBD	ASD	BSD(ours)
LC	CA	94.4	87.1	85.9	80.2	83.2	**93.9**	92.4
	ASR	99.9	24.4	50.5	1.6	98.1	73.2	**1.2**
	DER	-	84.1	70.5	92.1	45.3	63.1	**98.4**
SIG	CA	95.0	87.1	85.8	67.6	80.1	93.5	**93.8**
	ASR	95.2	60.8	83.0	5.1	99.9	96.5	**0.0**
	DER	-	63.3	51.5	81.4	42.6	49.3	**97.0**
ReFool	CA	95.2	86.5	85.6	76.3	**90.8**	86.8	**94.8**
	ASR	99.0	23.0	42.5	82.0	2.3	**0.4**	0.5
	DER	-	83.6	73.4	49.0	96.1	95.1	**99.0**
Narcissus	CA	95.2	87.2	86.5	79.3	87.3	93.9	**94.3**
	ASR	99.5	63.4	81.0	7.1	99.5	**0.0**	**0.0**
	DER	-	64.0	54.8	88.2	46.0	99.1	**99.3**
Average DER		-	73.8	62.6	77.7	57.5	76.6	**98.4**

Table 3: The clean accuracy (CA%), attack success rate (ASR%), and defense effectiveness rating (DER%) on CIFAR-10 of different defenses using mobilenet v2 (Sandler et al., 2018) as the backbone.

Attack	Metric	Non	FP	NAD	ABL	DBD	ASD	BSD(ours)
BadNet	CA	94.3	77.9	78.5	79.7	65.5	**93.2**	91.1
	ASR	100.0	8.3	11.7	13.6	**0.0**	100.0	0.4
	DER	-	87.7	86.2	85.9	85.6	49.4	**98.2**
Blended	CA	94.0	75.9	76.0	67.3	69.0	87.1	**90.0**
	ASR	99.3	30.8	46.0	2.6	**0.0**	99.0	0.2
	DER	-	75.2	67.7	85.1	87.2	46.7	**97.6**
WaNet	CA	94.0	82.2	81.5	50.9	58.4	83.0	**90.1**
	ASR	95.7	2.4	3.2	**0.5**	12.4	97.7	0.6
	DER	-	90.7	90.0	76.1	73.9	44.5	**95.6**
Average DER		-	84.5	81.3	82.3	82.2	46.9	**97.1**

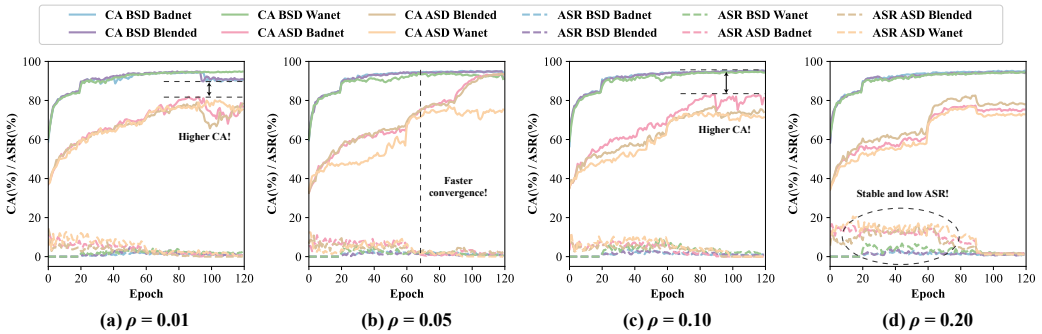

(a) $\rho = 0.01$ (b) $\rho = 0.05$ (c) $\rho = 0.10$ (d) $\rho = 0.20$

Figure 3: The performance of BSD in comparison with ASD (Gao et al., 2023) under different poisoning rates. The experiment is conducted on CIFAR-10 against three attacks.

5.5 Robustness to different poisoning rates

Despite the default poisoning rate $\rho = 0.05$ being a reasonable setting that is widely adopted in either backdoor attack or backdoor defense research (Huang et al., 2022; Gao et al., 2023; Min et al., 2024; Shi et al., 2023), it's crucial to verify the robustness of our BSD under different poisoning rates. As illustrated in Figure 3, although ASD performs well with respect to ASRs as well, the CAs of ASD are conspicuously lower under non-default settings. However, our BSD consistently achieves close-to-zero ASRs and satisfying CAs, emphasizing its robustness to different poisoning rates.

5.6 Training cost

Our BSD incorporates an altruistic model to assist with pool initialization and updates, which may raise concerns about increased training costs. However, as shown in Table 4, the training cost of BSD is comparable to, or even lower than, that of ASD (Gao et al., 2023). This is due to three key factors: 1) The altruistic model is updated through standard training rather than MixMatch, significantly

reducing time. 2) The altruistic model is only updated before stage 3, and its training primarily runs in parallel with the main model. 3) An imbalanced pool size, as seen in the early stages of ASD, often triggers frequent dataloader updates in MixMatch, whereas the clean pool size in BSD is more balanced and suitable during training.

Table 4: Training cost (hours) of ASD, DBD, and BSD on CIFAR-10, GTSRB, and Imagenet.

METHOD	CIFAR-10	GTSRB	IMAGENET	**AVERAGE**
DBD	11.96	10.09	53.21	25.09
ASD	4.81	2.55	12.09	6.48
BSD(OURS)	3.15	2.84	9.20	5.06

5.7 ABLATION STUDIES

Effectiveness of different stages. The major components of BSD are divided into pool initialization and pool updates. We investigated the significance of each component on CIFAR-10 to demonstrate their necessity, as shown in Table 5. OSS and ALS initialization are critical for avoiding backdoor overfitting (ASR); class completion update helps prevent class underfitting (CA); and selective dropping update acts as a final step to further reduce ASR, thereby achieving a higher DER.

Table 5: The ablation study on the strategies involved in BSD under CIFAR-10. 'Default' represents the result using all the proposed mechanisms, 'w/o Init' represents the results using random initialization. 'w/o Completion' represents disabling class completion in both stages 2 and 3. 'w/o Drop' represents disabling selective drop in stage 3.

SETTING↓	BADNET			BLENDED			WANET		
	CA	ASR	DER	CA	ASR	DER	CA	ASR	DER
DEFAULT	95.1	0.9	99.6	94.9	0.8	98.8	94.5	0.8	99.6
W/O INIT	94.7	100.0	49.9	95.0	99.2	49.6	93.6	91.5	54.2
W/O COMPLETION	90.7	0.0	97.9	86.8	0	95.5	89.8	0.2	98.0
W/O DROP	94.6	1.1	99.3	94.2	1.1	98.6	94.5	1.9	99.0

Influence of parameters. We here present the influence of the main parameter, i.e., the parameters α & β for pool size control. As revealed in Table 6, the performance is good near the default setting, while an extreme setting will lead to degradation on DER.

Table 6: Performance of BSD under different α & β on CIFAR-10. The results that have more than 0.5% DER decrease are marked using ↓.

SETTING↓	BADNET			BLENDED			WANET		
	CA	ASR	DER	CA	ASR	DER	CA	ASR	DER
DEFAULT	95.1	0.9	99.6	94.9	0.8	98.8	94.5	0.8	99.6
$\alpha = 0.3,\ \beta = 0.2$	94.9	1.2	99.4	94.8	0.6	98.9	94.2	1.8	99.1↓
$\alpha = 0.4,\ \beta = 0.2$	95.0	1.2	99.4	94.7	0.9	98.7	94.4	1.4	99.3
$\alpha = 0.5,\ \beta = 0.2$	95.0	1.7	99.2	94.2	0.8	98.7	94.7	1.4	99.2
$\alpha = 0.7,\ \beta = 0.2$	95.2	0.8	99.6	95.1	0.5	98.9	93.0	0.1	99.6
$\alpha = 0.8,\ \beta = 0.2$	95.0	1.1	99.5	92.8	0.5	98.2↓	91.7	1.0	98.5↓
$\alpha = 0.9,\ \beta = 0.2$	93.6	0.7	99.0↓	90.3	0.2	97.2↓	90.0	0.9	97.7↓
$\alpha = 0.6,\ \beta = 0.1$	94.8	0.7	99.6	90.9	0.5	97.3↓	91.6	0.6	98.7↓
$\alpha = 0.6,\ \beta = 0.3$	94.9	1.2	99.4	94.7	0.8	98.8	94.5	0.8	99.6
$\alpha = 0.6,\ \beta = 0.5$	94.7	1.4	99.2	94.9	1.6	98.4	94.3	2.3	98.8↓
$\alpha = 0.7,\ \beta = 0.7$	94.4	1.7	98.9↓	94.3	3.7	97.3↓	94.0	32.8	83.6↓

5.8 OTHER EXPERIMENTS

Additional experimental results, including visualizations, extended ablation studies, potential adaptive attacks, performance in the absence of attacks, the OSS distance metric, and more, are provided in Appendix E.

6 CONCLUSION

In conclusion, our proposed BSD effectively mitigates backdoor attacks through bi-perspective splitting mechanisms, without relying on on extra clean data. By leveraging OSS and ALS for robust dataset splitting, combined with class completion and selective dropping strategies, BSD achieves superior backdoor defense performance. Extensive experiments confirm BSD's robustness under different attack/defense settings.

REFERENCES

Jean-Baptiste Alayrac, Jonathan Uesato, Po-Sen Huang, Alhussein Fawzi, Robert Stanforth, and Pushmeet Kohli. Are labels required for improving adversarial robustness? *Advances in Neural Information Processing Systems*, 32, 2019.

Mauro Barni, Kassem Kallas, and Benedetta Tondi. A new backdoor attack in cnns by training set corruption without label poisoning. In *2019 IEEE International Conference on Image Processing (ICIP)*, pp. 101–105. IEEE, 2019.

Abhijit Bendale and Terrance E Boult. Towards open set deep networks. In *Proceedings of the IEEE conference on computer vision and pattern recognition*, pp. 1563–1572, 2016.

David Berthelot, Nicholas Carlini, Ekin D Cubuk, Alex Kurakin, Kihyuk Sohn, Han Zhang, and Colin Raffel. Remixmatch: Semi-supervised learning with distribution matching and augmentation anchoring. In *International Conference on Learning Representations*, 2019a.

David Berthelot, Nicholas Carlini, Ian Goodfellow, Nicolas Papernot, Avital Oliver, and Colin A Raffel. Mixmatch: A holistic approach to semi-supervised learning. *Advances in neural information processing systems*, 32, 2019b.

Eitan Borgnia, Valeriia Cherepanova, Liam Fowl, Amin Ghiasi, Jonas Geiping, Micah Goldblum, Tom Goldstein, and Arjun Gupta. Strong data augmentation sanitizes poisoning and backdoor attacks without an accuracy tradeoff. In *ICASSP 2021-2021 IEEE International Conference on Acoustics, Speech and Signal Processing (ICASSP)*, pp. 3855–3859. IEEE, 2021.

Nicholas Carlini and David Wagner. Towards evaluating the robustness of neural networks. In *2017 ieee symposium on security and privacy (sp)*, pp. 39–57. Ieee, 2017.

Yair Carmon, Aditi Raghunathan, Ludwig Schmidt, John C Duchi, and Percy S Liang. Unlabeled data improves adversarial robustness. *Advances in neural information processing systems*, 32, 2019.

Weixin Chen, Baoyuan Wu, and Haoqian Wang. Effective backdoor defense by exploiting sensitivity of poisoned samples. *Advances in Neural Information Processing Systems*, 35:9727–9737, 2022a.

Weixin Chen, Baoyuan Wu, and Haoqian Wang. Effective backdoor defense by exploiting sensitivity of poisoned samples. *Advances in Neural Information Processing Systems*, 35:9727–9737, 2022b.

Xinyun Chen, Chang Liu, Bo Li, Kimberly Lu, and Dawn Song. Targeted backdoor attacks on deep learning systems using data poisoning. *arXiv preprint arXiv:1712.05526*, 2017.

Jia Deng, Wei Dong, Richard Socher, Li-Jia Li, Kai Li, and Li Fei-Fei. Imagenet: A large-scale hierarchical image database. In *2009 IEEE conference on computer vision and pattern recognition*, pp. 248–255. Ieee, 2009.

Min Du, Ruoxi Jia, and Dawn Song. Robust anomaly detection and backdoor attack detection via differential privacy. *arXiv preprint arXiv:1911.07116*, 2019.

Mark Everingham, SM Ali Eslami, Luc Van Gool, Christopher KI Williams, John Winn, and Andrew Zisserman. The pascal visual object classes challenge: A retrospective. *International journal of computer vision*, 111:98–136, 2015.

Kuofeng Gao, Yang Bai, Jindong Gu, Yong Yang, and Shu-Tao Xia. Backdoor defense via adaptively splitting poisoned dataset. In *Proceedings of the IEEE/CVF Conference on Computer Vision and Pattern Recognition*, pp. 4005–4014, 2023.

Yudong Gao, Honglong Chen, Peng Sun, Zhe Li, Junjian Li, and Huajie Shao. Energy-based backdoor defense without task-specific samples and model retraining. In *Forty-first International Conference on Machine Learning*, 2024.

Micah Goldblum, Dimitris Tsipras, Chulin Xie, Xinyun Chen, Avi Schwarzschild, Dawn Song, Aleksander Madry, Bo Li, and Tom Goldstein. Dataset security for machine learning: Data poisoning, backdoor attacks, and defenses. *IEEE Transactions on Pattern Analysis and Machine Intelligence*, 45(2):1563–1580, 2022.

Tianyu Gu, Brendan Dolan-Gavitt, and Siddharth Garg. Badnets: Identifying vulnerabilities in the machine learning model supply chain. *arXiv preprint arXiv:1708.06733*, 2017.

Jiyang Guan, Jian Liang, and Ran He. Backdoor defense via test-time detecting and repairing. In *Proceedings of the IEEE/CVF Conference on Computer Vision and Pattern Recognition*, pp. 24564–24573, 2024.

Kaiming He, Xiangyu Zhang, Shaoqing Ren, and Jian Sun. Deep residual learning for image recognition. In *Proceedings of the IEEE conference on computer vision and pattern recognition*, pp. 770–778, 2016.

Shengshan Hu, Ziqi Zhou, Yechao Zhang, Leo Yu Zhang, Yifeng Zheng, Yuanyuan He, and Hai Jin. Badhash: Invisible backdoor attacks against deep hashing with clean label. In *Proceedings of the 30th ACM international conference on Multimedia*, pp. 678–686, 2022.

Binxiao Huang, Jason Chun Lok, Chang Liu, and Ngai Wong. Poisoning-based backdoor attacks for arbitrary target label with positive triggers. *arXiv preprint arXiv:2405.05573*, 2024.

Kunzhe Huang, Yiming Li, Baoyuan Wu, Zhan Qin, and Kui Ren. Backdoor defense via decoupling the training process. *arXiv preprint arXiv:2202.03423*, 2022.

Andrew Ilyas, Logan Engstrom, Anish Athalye, and Jessy Lin. Black-box adversarial attacks with limited queries and information. In *International conference on machine learning*, pp. 2137–2146. PMLR, 2018.

Alex Krizhevsky, Geoffrey Hinton, et al. Learning multiple layers of features from tiny images. 2009.

Alexey Kurakin, Ian J Goodfellow, and Samy Bengio. Adversarial examples in the physical world. In *Artificial intelligence safety and security*, pp. 99–112. Chapman and Hall/CRC, 2018.

Shaofeng Li, Minhui Xue, Benjamin Zi Hao Zhao, Haojin Zhu, and Xinpeng Zhang. Invisible backdoor attacks on deep neural networks via steganography and regularization. *IEEE Transactions on Dependable and Secure Computing*, 18(5):2088–2105, 2020.

Yige Li, Xixiang Lyu, Nodens Koren, Lingjuan Lyu, Bo Li, and Xingjun Ma. Anti-backdoor learning: Training clean models on poisoned data. *Advances in Neural Information Processing Systems*, 34: 14900–14912, 2021a.

Yige Li, Xixiang Lyu, Nodens Koren, Lingjuan Lyu, Bo Li, and Xingjun Ma. Neural attention distillation: Erasing backdoor triggers from deep neural networks. *arXiv preprint arXiv:2101.05930*, 2021b.

Yige Li, Xixiang Lyu, Xingjun Ma, Nodens Koren, Lingjuan Lyu, Bo Li, and Yu-Gang Jiang. Reconstructive neuron pruning for backdoor defense. *arXiv preprint arXiv:2305.14876*, 2023a.

Yiming Li, Yong Jiang, Zhifeng Li, and Shu-Tao Xia. Backdoor learning: A survey. *IEEE Transactions on Neural Networks and Learning Systems*, 2022.

Yiming Li, Mengxi Ya, Yang Bai, Yong Jiang, and Shu-Tao Xia. BackdoorBox: A python toolbox for backdoor learning. In *ICLR Workshop*, 2023b.

Kang Liu, Brendan Dolan-Gavitt, and Siddharth Garg. Fine-pruning: Defending against backdooring attacks on deep neural networks. In *International symposium on research in attacks, intrusions, and defenses*, pp. 273–294. Springer, 2018.

Min Liu, Alberto Sangiovanni-Vincentelli, and Xiangyu Yue. Beating backdoor attack at its own game. In *Proceedings of the IEEE/CVF International Conference on Computer Vision*, pp. 4620–4629, 2023.

Yunfei Liu, Xingjun Ma, James Bailey, and Feng Lu. Reflection backdoor: A natural backdoor attack on deep neural networks. In *Computer Vision–ECCV 2020: 16th European Conference, Glasgow, UK, August 23–28, 2020, Proceedings, Part X 16*, pp. 182–199. Springer, 2020.

Rui Min, Zeyu Qin, Li Shen, and Minhao Cheng. Towards stable backdoor purification through feature shift tuning. *Advances in Neural Information Processing Systems*, 36, 2024.

Seyed-Mohsen Moosavi-Dezfooli, Alhussein Fawzi, and Pascal Frossard. Deepfool: a simple and accurate method to fool deep neural networks. In *Proceedings of the IEEE conference on computer vision and pattern recognition*, pp. 2574–2582, 2016.

Anh Nguyen and Anh Tran. Wanet–imperceptible warping-based backdoor attack. *arXiv preprint arXiv:2102.10369*, 2021.

Minzhou Pan, Yi Zeng, Lingjuan Lyu, Xue Lin, and Ruoxi Jia. {ASSET}: Robust backdoor data detection across a multiplicity of deep learning paradigms. In *32nd USENIX Security Symposium (USENIX Security 23)*, pp. 2725–2742, 2023.

Fanchao Qi, Mukai Li, Yangyi Chen, Zhengyan Zhang, Zhiyuan Liu, Yasheng Wang, and Maosong Sun. Hidden killer: Invisible textual backdoor attacks with syntactic trigger. *arXiv preprint arXiv:2105.12400*, 2021.

Mark Sandler, Andrew Howard, Menglong Zhu, Andrey Zhmoginov, and Liang-Chieh Chen. Mobilenetv2: Inverted residuals and linear bottlenecks. In *Proceedings of the IEEE conference on computer vision and pattern recognition*, pp. 4510–4520, 2018.

Ali Shafahi, W Ronny Huang, Mahyar Najibi, Octavian Suciu, Christoph Studer, Tudor Dumitras, and Tom Goldstein. Poison frogs! targeted clean-label poisoning attacks on neural networks. *Advances in neural information processing systems*, 31, 2018.

Yucheng Shi, Mengnan Du, Xuansheng Wu, Zihan Guan, Jin Sun, and Ninghao Liu. Black-box backdoor defense via zero-shot image purification. *Advances in Neural Information Processing Systems*, 36:57336–57366, 2023.

Kihyuk Sohn, David Berthelot, Nicholas Carlini, Zizhao Zhang, Han Zhang, Colin A Raffel, Ekin Dogus Cubuk, Alexey Kurakin, and Chun-Liang Li. Fixmatch: Simplifying semi-supervised learning with consistency and confidence. *Advances in neural information processing systems*, 33:596–608, 2020.

J. Stallkamp, M. Schlipsing, J. Salmen, and C. Igel. Man vs. computer: Benchmarking machine learning algorithms for traffic sign recognition. *Neural Networks*, (0):–, 2012. ISSN 0893-6080. doi: 10.1016/j.neunet.2012.02.016. URL `http://www.sciencedirect.com/science/article/pii/S0893608012000457`.

Indranil Sur, Karan Sikka, Matthew Walmer, Kaushik Koneripalli, Anirban Roy, Xiao Lin, Ajay Divakaran, and Susmit Jha. Tijo: Trigger inversion with joint optimization for defending multimodal backdoored models. In *Proceedings of the IEEE/CVF International Conference on Computer Vision*, pp. 165–175, 2023.

Brandon Tran, Jerry Li, and Aleksander Madry. Spectral signatures in backdoor attacks. *Advances in neural information processing systems*, 31, 2018.

Alexander Turner, Dimitris Tsipras, and Aleksander Madry. Clean-label backdoor attacks. 2018.

Alexander Turner, Dimitris Tsipras, and Aleksander Madry. Label-consistent backdoor attacks. *arXiv preprint arXiv:1912.02771*, 2019.

Hongyi Wang, Kartik Sreenivasan, Shashank Rajput, Harit Vishwakarma, Saurabh Agarwal, Jy-yong Sohn, Kangwook Lee, and Dimitris Papailiopoulos. Attack of the tails: Yes, you really can backdoor federated learning. *Advances in Neural Information Processing Systems*, 33:16070–16084, 2020.

Yisen Wang, Xingjun Ma, Zaiyi Chen, Yuan Luo, Jinfeng Yi, and James Bailey. Symmetric cross entropy for robust learning with noisy labels. In *Proceedings of the IEEE/CVF international conference on computer vision*, pp. 322–330, 2019.

Maurice Weber, Xiaojun Xu, Bojan Karlaš, Ce Zhang, and Bo Li. Rab: Provable robustness against backdoor attacks. In *2023 IEEE Symposium on Security and Privacy (SP)*, pp. 1311–1328. IEEE, 2023.

Emily Wenger, Josephine Passananti, Arjun Nitin Bhagoji, Yuanshun Yao, Haitao Zheng, and Ben Y Zhao. Backdoor attacks against deep learning systems in the physical world. In *Proceedings of the IEEE/CVF conference on computer vision and pattern recognition*, pp. 6206–6215, 2021.

Baoyuan Wu, Hongrui Chen, Mingda Zhang, Zihao Zhu, Shaokui Wei, Danni Yuan, and Chao Shen. Backdoorbench: A comprehensive benchmark of backdoor learning. *Advances in Neural Information Processing Systems*, 35:10546–10559, 2022.

Dongxian Wu and Yisen Wang. Adversarial neuron pruning purifies backdoored deep models. *Advances in Neural Information Processing Systems*, 34:16913–16925, 2021.

Qizhe Xie, Zihang Dai, Eduard Hovy, Thang Luong, and Quoc Le. Unsupervised data augmentation for consistency training. *Advances in neural information processing systems*, 33:6256–6268, 2020.

Xiaohui Zeng, Chenxi Liu, Yu-Siang Wang, Weichao Qiu, Lingxi Xie, Yu-Wing Tai, Chi-Keung Tang, and Alan L Yuille. Adversarial attacks beyond the image space. In *Proceedings of the IEEE/CVF Conference on Computer Vision and Pattern Recognition*, pp. 4302–4311, 2019.

Yi Zeng, Si Chen, Won Park, Z Morley Mao, Ming Jin, and Ruoxi Jia. Adversarial unlearning of backdoors via implicit hypergradient. *arXiv preprint arXiv:2110.03735*, 2021.

Yi Zeng, Minzhou Pan, Himanshu Jahagirdar, Ming Jin, Lingjuan Lyu, and Ruoxi Jia. {Meta-Sift}: How to sift out a clean subset in the presence of data poisoning? In *32nd USENIX Security Symposium (USENIX Security 23)*, pp. 1667–1684, 2023a.

Yi Zeng, Minzhou Pan, Hoang Anh Just, Lingjuan Lyu, Meikang Qiu, and Ruoxi Jia. Narcissus: A practical clean-label backdoor attack with limited information. In *Proceedings of the 2023 ACM SIGSAC Conference on Computer and Communications Security*, pp. 771–785, 2023b.

Zaixi Zhang, Jinyuan Jia, Binghui Wang, and Neil Zhenqiang Gong. Backdoor attacks to graph neural networks. In *Proceedings of the 26th ACM Symposium on Access Control Models and Technologies*, pp. 15–26, 2021.

Zaixi Zhang, Qi Liu, Zhicai Wang, Zepu Lu, and Qingyong Hu. Backdoor defense via deconfounded representation learning. In *Proceedings of the IEEE/CVF Conference on Computer Vision and Pattern Recognition*, pp. 12228–12238, 2023.

Mingli Zhu, Shaokui Wei, Li Shen, Yanbo Fan, and Baoyuan Wu. Enhancing fine-tuning based backdoor defense with sharpness-aware minimization. In *Proceedings of the IEEE/CVF International Conference on Computer Vision*, pp. 4466–4477, 2023a.

Mingli Zhu, Shaokui Wei, Hongyuan Zha, and Baoyuan Wu. Neural polarizer: A lightweight and effective backdoor defense via purifying poisoned features. *Advances in Neural Information Processing Systems*, 36, 2024.

Xiaojin Zhu and Andrew B Goldberg. *Introduction to semi-supervised learning*. Springer Nature, 2022.

Zixuan Zhu, Rui Wang, Cong Zou, and Lihua Jing. The victim and the beneficiary: Exploiting a poisoned model to train a clean model on poisoned data. In *Proceedings of the IEEE/CVF International Conference on Computer Vision*, pp. 155–164, 2023b.

A Extended discussions

A.1 Extended related works

With the advance of clean subset extraction and backdoor detection, many works tries to split clean subset from poison training sets. Zeng et al. (2023a) proposed detecting poisoned data by identifying shifts in data distributions, which results in high prediction loss when training on the clean portion of a poisoned dataset and testing on the corrupted portion. They solve a relaxed of the splitting optimization problem with the help of a weight-assigning network. Although promising empirical results were presented, the proposed META-SIFT only guarantees a relatively small subset ((Zeng et al., 2023a), page 10, Figure 5). As a result, META-SIFT still relies on effective downstream defenses, such as NAD and ASD, included in our baselines, while also increasing the hyperparameter search space. Pan et al. (2023) are motivated by the same distributional shift phenomenon and proposed an effective splitting algorithm, ASSET. However, they assume that the defender has an extra set of clean samples (named "base set" in (Pan et al., 2023)), which doesn't suit the background of our paper, where no extra clean set is available. Plus, ASSET is faced with the same problem that requires effective downstream defenses to conduct the defense.

In general, these works indeed provide valuable insights into the poisoned data splitting problem and could inspire our future research. However, they are faced with two major problems. 1) Cannot guarantee a 100% correct split that can be directly used for training; 2) Rely on an extra clean set which violates the constraints of our scenario.

A.2 Additional baselines

We added two recent defense, VaB (Zhu et al., 2023b) and D-ST/D-BR (Chen et al., 2022b). The additional baselines are implemented based on the official implementation. We use CIFAR-10 as the dataset. Since the label-consistent attack is not consistently implemented, we use SIG as a clean label attack here. As shown in Table 7, VaB has the most competitive result against poison label attacks, but struggles to defend against SIG.

Table 7: The clean accuracy (CA%), attack success rate (ASR%), defense effective rating (DER%) and time cost (hours) of 2 additional backdoor defense methods and our BSD against 4 threatening backdoor attacks on CIFAR-10. The best and second best results are in **bold** and underlined.

Method	Badnets			Blended			WaNet			SIG			Avg	Time
	CA	ASR	DER	CA	ASR	DER	CA	ASR	DER	CA	ASR	DER	DER	Cost
VaB	94.0	1.3	98.9	94.2	1.1	98.6	93.6	1.7	99.1	94.0	66.6	63.8	90.1	5.5
D-ST	66.8	5.7	83.1	65.0	7.1	81.1	60.8	15.2	76.0	87.9	95.1	46.5	71.6	4.3
D-BR	87.5	**0.8**	95.9	83.0	80.7	53.2	16.9	14.6	54.3	85.7	0.1	92.9	74.1	-
BSD(Ours)	**95.1**	0.9	**99.6**	**94.9**	**0.8**	**98.8**	**94.5**	**0.8**	**99.6**	**93.8**	**0.0**	**97.0**	**98.7**	**3.2**

A.3 Discussion on resistance to clean-label attack

The primary reason BSD can effectively resist clean-label backdoor attacks lies in how the MixMatch algorithm processes unlabeled data. Specifically, MixMatch applies a mixup operation that visually weakens the trigger and prevents it from being directly associated with the target label.

To better understand this phenomenon, we analyzed related semi-supervised defense methods like ASD. ASD report good performance against label-consistent attacks. In successful cases of ASD, poison samples were correctly classified into the poison pool, while failures often occurred when poison samples remained in the clean pool (Table 8).

Table 8: Number of poison samples in the clean pool of failed runs of ASD (CIFAR-10, LC attack, poisoning ratio 2.5%). The number of poison sample in clean pool exceeds 500 in average (poisoning ratio 2% in clean pool), which is the main reason that it fails to resist LC attack.

Epoch→	111	112	113	114	115	116	117	118	119	120	mean	std
NumOfPoison(run 1)	405	567	683	321	695	280	303	595	391	910	515	208.4
NumOfPoison(run 2)	936	466	838	544	658	146	435	370	530	345	526.8	234.9

This led us to hypothesize that the key factor influencing clean-label attack defense is still the accurate classification of poison samples into the poison pool. Further investigation revealed that the mixup operation in MixMatch plays a critical role. MixMatch not only removes original labels but also mixes multiple inputs on the image level, effectively weakening the visual impact of the trigger. We visualized the mixed samples together with the argmaxed mixed label in Figure 4 to better present the mixup operation.

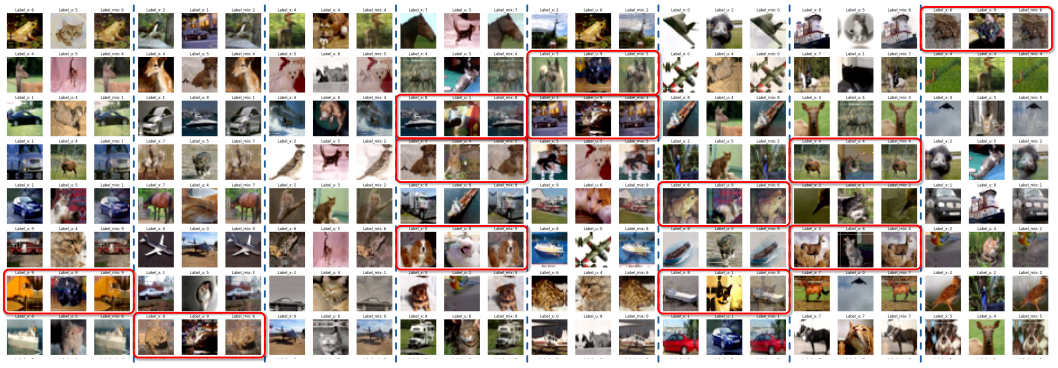

Figure 4: Visualization of the mixup operation in MixMatch. We take a random batch at the end of training of our BSD against LC attack on CIFAR-10. Each group of three pictures has labeled data on the left (original label), unlabeled data in the middle (predicted label by the model), and mixed data on the right (mixed label).

Because of $\alpha = 0.75$ in the default setting of MixMatch, λ' has a mathematical expectation of approximately 0.78, the mixed inputs diminish the prominence of the trigger in x_u. We visualized the mixed samples together with to better present the mixup operation. Furthermore, we follow ASD to set a 5 times smaller λ_u value (15 vs. MixMatch's recommended 75), reducing the influence of unlabeled data and further mitigating clean-label attacks.

Finally, to verify this hypothesis, we manually enforced a secure clean-poison split where no poison samples were included in the clean pool. Under this condition, MixMatch effectively nullified the impact of clean-label attacks, as shown in Table 9.

Table 9: Train with MixMatch and secured clean pool against clean label attacks.

Method	LC-CIFAR			LC-GTSRB			SIG-CIFAR			Narcissus_CIFAR		
	CA	ASR	DER	CA	ASR	DER	CA	ASR	DER	CA	ASR	DER
No Defense	94.4	99.9	-	97.3	100.0	-	95.0	95.2	-	95.2	99.5	-
MixMatch*	94.2	0.0	99.9	97.4	0.0	100.0	94.6	0.0	97.4	94.5	0.0	99.3

A.4 Robustness against different targets

We evaluated the robustness against different targets of our BSD in Table 10

Table 10: The clean accuracy (CA%), attack success rate (ASR%), and defense effective rating (DER%) of our BSD against 3 representitive backdoor attacks with different target labels on CIFAR-10.

Target	BadNets			Blended			WaNet		
	CA	ASR	DER	CA	ASR	DER	CA	ASR	DER
0	95.0	0.8	99.6	95.0	0.4	99.0	91.9	0.3	99.0
1	94.9	0.5	99.8	94.9	0.5	98.9	94.2	0.3	99.8
2	95.1	0.8	99.6	94.7	0.9	98.7	90.9	0.7	98.3
3	95.1	0.9	99.6	94.9	0.8	98.8	94.5	0.8	99.6
4	95.0	0.2	99.9	94.8	0.6	98.9	92.4	0.2	99.3
5	95.1	1.7	99.2	95.0	0.5	98.9	91.9	0.4	98.9
6	95.1	0.6	99.7	93.9	0.6	98.8	92.6	0.3	99.3
7	94.7	0.3	99.8	92.6	0.4	98.2	90.3	0.0	98.3
8	92.0	0.3	98.4	95.1	0.5	98.9	91.8	0.3	98.9
9	94.9	0.3	99.8	94.0	0.4	98.9	94.0	0.2	99.9
Avg	94.7	0.6	99.5	94.5	0.6	98.8	92.5	0.4	99.1

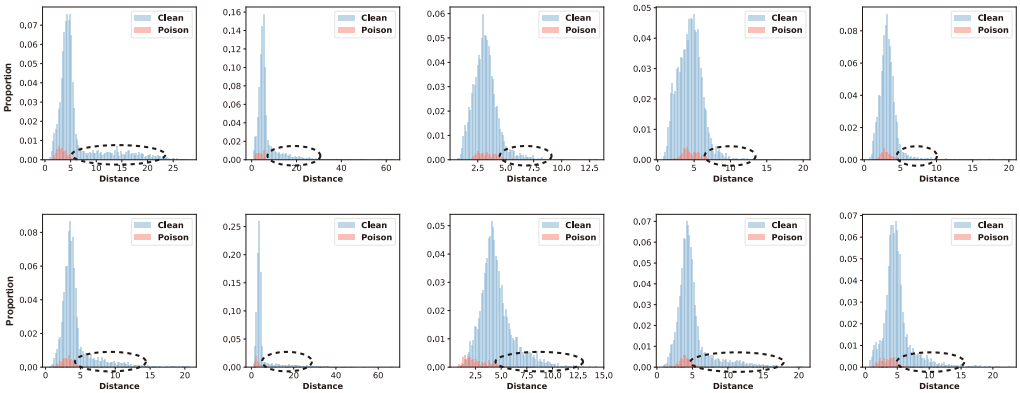

Figure 5: Visiualization fo the effectiveness of OSS against BadNet-all2all attack.

A.5 Robustness against all2all attacks

All-to-all (all2all) attacks may pose challenges to certain components of our defense, particularly OSS and selective drop. However, all2all attacks are not typically considered essential scenarios in backdoor defense research currently (Li et al., 2021a; Huang et al., 2022; Zhu et al., 2023b; Guan et al., 2024; Zhang et al., 2023), for the following reasons: 1) The increased number of trigger-target pairs in all2all attacks requires significantly more training epochs for success. And all2all attacks reduce clean accuracy and exhibit slower convergence, making them easier to detect. (Huang et al. (2024), Page 2: "As the number of classes increases, the accuracy and the attack success rate will decrease.") 2) Research on all2all attacks remains limited (Li et al. (2022), Page 10: "However, there were only a few studies on all-to-all attacks. How to better design the all-to-all attack and the analysis of its properties remain blank."). 3) In practical applications, all2all attacks do not allow attackers to arbitrarily control predictions to specific targets, limiting their real-world threat.

Nevertheless, we still conducted supplementary experiments on BadNets with an all2all setting.

Attack setting: Following BadNets, with $y_t = (y + 1)\%n_c$, where n_c is the number of classes.

Defense setting: To handle multiple target labels, BSD incurs additional computational costs by iterating through all classes as pseudo-targets during OSS. Clean indices from each pseudo-target are intersected to form the final OSS result. Additionally, we early stop at Stage 2 to avoid meaningless cost in Stage 3.

Since all-to-all attacks do not fundamentally change the nature of poison-label attacks, OSS remains effective for each individual classes. We visualized OSS spliting results in Figure 5, which reveals effective separation of clean samples of OSS. The CA, ASR, and DER performance are presented in Table 11, demonstrating a significant DER improvement compared to baseline methods. Notably, while BSD's ASR increases under all-to-all attacks, it effectively limits the attack success rate to the level of random prediction ($1/n_c = 10\%$).

In conclusion, our BSD method remains effective against all-to-all attacks. Furthermore, the OSS module can serve as a highly effective component for identifying clean samples in other backdoor defense methods.

Table 11: The clean accuracy (CA%), attack success rate (ASR%), and defense effective rating (DER%) of ASD and our BSD against BadNets-all2all on CIFAR-10.

Method	BadNets-all2all		
	CA	ASR	DER
No Defense	91.8	93.8	-
ASD	70.2	2.4	84.9
BSD (Ours)	91.2	10.5	91.3

A.6 PSEUDO TARGET APPROXIMATION TEST

Pseudo target approximation test on GTSRB. We evaluated the approximation of y_t on the GTSRB dataset with various ground truth target labels, as shown in Table 12 (using the alternative approximation method described in Appendix E.3). The results demonstrate that y_t was successfully approximated for all of the first 10 classes in GTSRB.

Table 12: Testing the y_t approximation on different target labels (the first 10 classes) on GTSRB.

ATTACK	0	1	2	3	4	5	6	7	8	9
BADNETS	✓	✓	✓	✓	✓	✓	✓	✓	✓	✓
BLENDED	✓	✓	✓	✓	✓	✓	✓	✓	✓	✓
LC	✓	✓	✓	✓	✓	✓	✓	✓	✓	✓

Performance under forced incorrect pseudo target label. We conducted interesting additional tests by forcing y_t to be assigned to an incorrect class and observed the model's performance (on CIFAR-10, against BadNets). As illustrated in Figure 6, BSD retained partial defensive capabilities even when the pseudo-label was deliberately set incorrectly. In most cases presented, BSD managed to purify the model successfully, leveraging the loss-guided splitting based on the Altruistic model.

It is worth noting that in experiments where the ground truth target class was 5 (dog), forcibly setting the pseudo-label to 3 (cat) led to a significant failure of the defense. This may be attributed to the inherent difficulty in distinguishing between these two classes. Furthermore, when faced with broader attack scenarios and dataset settings, relying solely on loss statistics may not be sufficient to ensure effective defense. Fortunately, our experiments demonstrate the strong robustness of the proposed Pseudo Target Approximation method. The OSS mechanism functioned as expected, enabling a resilient bi-perspective defense under challenging conditions.

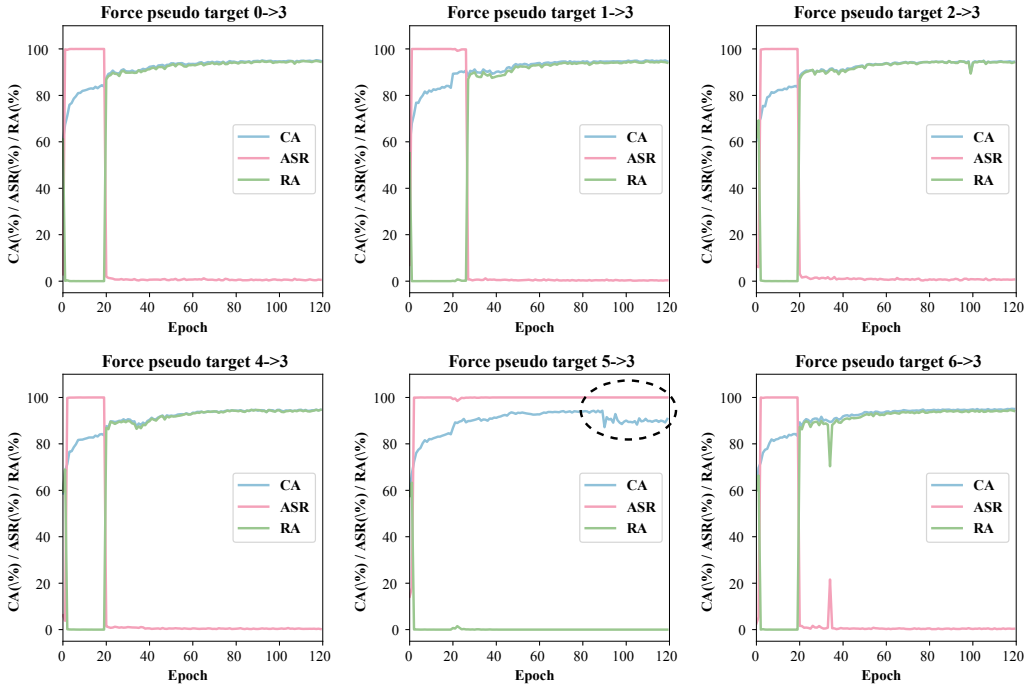

Figure 6: The clean accuracy (CA%), attack success rate (ASR%), and robust accuracy (RA%) of BSD when Forcing the pseudo target from x(ground truth) to 3.

B ALGORITHM OUTLINE

The pseudocode of the proposed method BSD is listed as Algorithm 1.

Algorithm 1 Pseudocode for BSD

Input: Poisoned training set $\mathcal{D}$; main model f; main model warm-up ends at epoch T_1, main model training stage2 ends at epoch T_2, main model training stage3 ends at epoch T_3, max clean pool ratio α, OSS split ratio β.
Output: Clean model $f_{\theta'}$

 # Initialization & warm-up
Initialize the weights of f as θ
Generate an altruistic model g having the same architecture as f, initialize the weights as φ
# Prepare for ALS
for i = 1 to 25 **do**
  for each sample (x, y) in $\mathcal{D}$ **do**
    $loss \leftarrow \mathcal{L}_{ce}(x, y, g_\varphi)$
    $loss \leftarrow \text{sign}(loss - 0.5) \times loss$ # Default LGA
    $\varphi \leftarrow \varphi - \nabla_\varphi loss$
  end for
end for
# Prepare for OSS
Set y_t as the most frequent class among the 1% lowest $\mathcal{L}_{ce}(g_\varphi)$ samples in $\mathcal{D}$
Calculate $\mathcal{D}_{\text{t}}$ and $\mathcal{D}_{\text{nt}}$ with y_t according to Section 3.2
 # Main Training Loop
while $T < T_3$ **do**
  if $T < T_1$ **then**
    # Data used for the main model warm-up
    $\mathcal{D}_c \leftarrow \mathcal{D}_{\text{nt}}$
  else if $T = T_1$ **then**
    # Pool initialization using ALS and OSS
    $\mathcal{D}_c \leftarrow \mathcal{D}_{\text{als}} \cup \mathcal{D}_{\text{oss}}$
  else if $T_1 + 10 \leq T < T_2$ **then**
    # Pool update based on loss discrepancy of f_θ and g_φ, enabling class completion
    $T' \leftarrow \frac{T - T_1 - 10}{T_2 - T_1 - 10} T_2$
    Current clean ratio $\alpha_T \leftarrow \beta + (\alpha - \beta) \times (1 - \cos(\pi \times T'/T_2))/2$
    Set α as α_T in equation 8
    Calculate $\mathcal{D}_{\tilde{c_1}}$ according to equation 8
    $\mathcal{D}_c \leftarrow \mathcal{D}_{\tilde{c_1}}$
  else if $T \geq T_2$ **then**
    # Pool update based on loss discrepancy of f_θ and g_φ, enabling class completion and selective drop
    Current clean ratio $\alpha_T \leftarrow \alpha$
    Set α as α_T in equation 10
    Calculate $\mathcal{D}_{\tilde{c_2}}$ according to equation 10
    $\mathcal{D}_c \leftarrow \mathcal{D}_{\tilde{c_2}}$
  end if
  $\mathcal{D}_p \leftarrow \mathcal{D} \setminus \mathcal{D}_c$
  # Models updating
  $\theta \leftarrow \theta - \nabla_\theta \mathcal{L}_{\text{semi}}$ # Train the model on $\mathcal{D}_c$(labeled) and $\mathcal{D}_p$ by semi-supervised learning
  if $T < T_2$ **then**
    $\varphi \leftarrow \varphi - \nabla_\varphi \mathcal{L}_{ce}$ # Train the altruistic model by supervised learning
  end if
end while

C IMPLEMENTATION DETAILS

C.1 ENVIRONMENTS

We run all the experiments using PyTorch on a Linux server with an AMD EPYC 7H12 64-core Processor, 256GB RAM, and 8× NVIDIA GeForce RTX 3090 GPU.

C.2 ILLUSTRATION OF THE POISONED SAMPLES

Figure 7 illustrates the seven attack types used in this study, displaying both the original and poisoned images along with the corresponding trigger patterns. For attacks involving a different trigger in the Imagenet dataset, the specific trigger is also shown at the bottom.

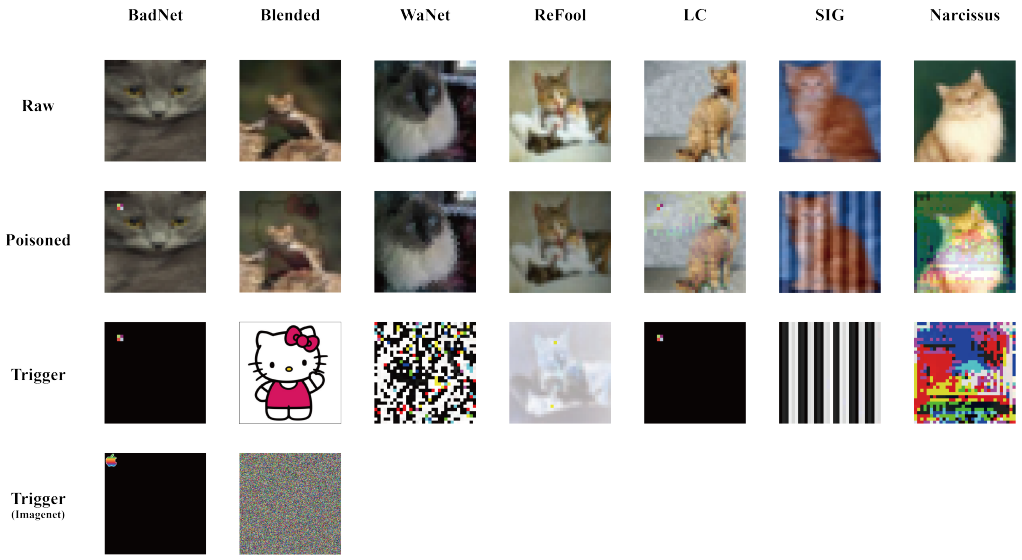

Figure 7: Illustation of the backdoor attacks. We present the examples on CIFAR-10, alternative triggers (if used) on Imagenet are shown at the bottom.

C.3 ATTACK SETTINGS

Training settings. For all the attack implementations, we follow that in ASD (Gao et al., 2023). On the CIFAR-10 and GTSRB datasets, we perform backdoor attacks on ResNet-18 for 200 epochs with batch size 128. We adopt the stochastic gradient descent (SGD) optimizer with a learning rate of 0.1, momentum of 0.9, and weight decay 5×10^{-4}. The learning rate is divided by 10 at epoch 100 and 150. For attacks not achieving reported performance in ASD (Gao et al., 2023), we continue the training for another 100 epochs, and the learning rate is divided by 10 at epoch 200 and 250. On the Imagenet (Deng et al., 2009) dataset, we train ResNet-18 for 90 epochs with batch size 256. We utilize the SGD optimizer with a learning rate of 0.1, momentum of 0.9, and weight decay 1×10^{-4}. The learning rate is decreased by a factor of 10 at epoch 30 and 60. The image resolution will be resized to $224 \times 224 \times 3$ before attaching the trigger pattern.

Settings for BadNets. As suggested by Gu et al. (2017); Huang et al. (2022); Gao et al. (2023), we set a 2×2 square on the upper left corner as the trigger pattern on CIFAR-10 and GTSRB. For ImageNet and VGGFace2, we use a 32×32 apple logo on the upper left corner. The poisoning rate ρ is set to 0.05(5%).

Settings for Blended. Following Chen et al. (2017); Huang et al. (2022); Gao et al. (2023), we choose"Hello Kitty" pattern on CIFAR-10 and GTSRB and the random noise pattern on ImageNet and VGGFace2. The blend ratio is set to 0.1. The poisoning rate ρ is set to 0.05(5%).

Settings for WaNet. Following Gao et al. (2023); Huang et al. (2022), we directly use the default warping-based operation to generate the trigger pattern. For CIFAR-10 and GTSRB, we set the noise

rate ρ_n to 0.2, control gird size k as 4, and warping strength s as 0.5. For Imagenet, we use the same noise rate, but a larger grid size $k = 224$, and a warping strength $s = 1$.

Settings for Label-Consistent Attack. Following Gao et al. (2023); Huang et al. (2022); Turner et al. (2019), the noisy versions of samples are generated using adversarially trained models. The PGD parameters are as follows: for PGD training: $\epsilon = 16$, $\alpha = 2$, steps = 7, and the pixel range is [0, 255]; for PGD attack: $\epsilon = 16$, $\alpha = 1.5$, steps = 30, with the same pixel range [0, 255]. The same trigger used in BadNets is applied for LC attacks, and the poison ratio is set at 25

Settings for Refool. Following Li et al. (2021a); Liu et al. (2020), we randomly choose 5,000 images from PascalVOC (Everingham et al., 2015) as the candidate reflection set $\mathcal{R}_{cand}$ and randomly choose one of the three reflection methods to generate the trigger pattern during the backdoor attack.

Settings for SIG. Following Li et al. (2021a); Barni et al. (2019), we adopt the same sinusoidal pattern in ABL as the trigger and set the poisoning rate to match LC, as SIG is a clean-label attack.

Settings for Narcissus. We also incorporate the recent attack proposed by Zeng et al. (2023b), which is another clean-label attack. The parameter settings for generating the Narcissus trigger pattern are as follows: the ℓ_∞ ball bound is set to 16/255, the surrogate model is trained for 200 epochs with an initial learning rate of 0.1 and a warm-up period of 5 rounds. The trigger-generation learning rate is 0.01, and the generation process lasts for 1000 rounds. The poisoning rate is the same as LC, given that Narcissus is also a clean-label attack.

C.4 Defense settings

Settings for FP. Following Gao et al. (2023), we set two steps of FP Liu et al. (2018) (i.e., pruning and fine-tuning) as follows. (1) We randomly select 5% clean training samples as the local clean samples and forward them to obtain the activation values of neurons in the last convolutional layer. The dormant neurons on clean samples with the lowest $\alpha\%$ activation values will be pruned. (2) The pruned model will be fine-tuned on the local clean samples for 10 epochs. In particular, the learning rate is set as 0.01, 0.01, 0.1 on CIFAR-10, GTSRB, and ImageNet. Unless otherwise specified, other settings are the same as those used by Liu et al. (2018). For the hyper-parameters of FP, we search for the best results by adjusting the pruned ratio $\alpha\% \in 20\%, 30\%, 40\%, 50\%, 60\%, 70\%, 80\%, 90\%$. In addition, we add another default setting in backdoorbench (Wu et al., 2022).

Settings for NAD. NAD (Li et al., 2021b) is also a post trianing method that repairs the backdoored model and needs 5% local clean training samples. We set the two steps of NAD as follows: (1) Use the local clean samples to fine-tune the backdoored model for 10 epochs. Specially, the learning rate is set as 0.01, 0.01, 0.1 on CIFAR-10, GTSRB, and ImageNet. (2) The fine-tuned model and the backdoored model will be regarded as the teacher model and student model to perform the distillation process. Unless otherwise specified, other settings are the same as those used by Li et al. (2021b). For the sensitive hyper-parameter β, we find the search space used by Gao et al. (2023) too small. We search for the best results by adjusting the hyper-parameter β from 500, 1000, 1500, 2000, 2500, 5000, 7500, 1e5, 1e6, 1e7, 1e8, 1e9, 1e10, 1e11. In addition, we add another default setting in backdoorbench (Wu et al., 2022).

Settings for ABL. ABL (Li et al., 2021a) contains three stages: (1) To obtain the poisoned samples, ABL first trains the model on the poisoned dataset for 20 epochs by LGA loss and isolate 1% training samples with the lowest loss. (2) Continue to train the model with the poisoned dataset after the backdoor isolation for 70 epochs. (3) Finally, the model will be unlearned by the isolation samples for 5 epochs. The learning rate is 5e-4 at the unlearning stage. Unless otherwise specified, other settings are the same as those used by Li et al. (2021a). ABL is sensitive to the hyper-parameter γ in LGA loss. We search for the best results by adjusting the hyper-parameter γ from 0, 0.1, 0.2, 0.3, 0.4, 0.5, In addition, we add another default setting in backdoorbench (Wu et al., 2022).

Settings for DBD. DBD (Huang et al., 2022) contains three independent stages: (1) DBD uses SimCLR to perform the self-supervised learning for 1,000 epochs. (2) Freeze the backbone and fine-tune the linear layer by supervised learning for 10 epochs. (3) Adopt the MixMatch to conduct the semi-supervised learning for 200 epochs on CIFAR-10 and GTSRB for 90 epochs on ImageNet and VGGFace2. Unless otherwise specified, other settings are the same as those used by Huang et al. (2022). Since DBD is a relatively stable backdoor defense and not sensitive to its hyper-parameter, we only add another group of default setting in backdoorbench (Wu et al., 2022).

Settings for ASD. We follow the exact settings for ASD as suggested by Gao et al. (2023). To name a few settings, we adopt MixMatch as the semi-supervised learning framework and use the Adam optimizer with a learning rate of 0.002 and a batch size of 64 for the semi-supervised training. The temperature T is set to 0.5, and the weight of the unsupervised loss λ_u is set to 15. The training stages are defined as follows: $T_1 = 60$, $T_2 = 90$, and $T_3 = 120$ for CIFAR-10 and ImageNet, while $T_3 = 100$ for GTSRB. Similarly, other parameters are the same as used by Gao et al. (2023) as well.

For our BSD, we adopt the MixMatch Berthelot et al. (2019b) semi-supervised training framework for the main model, following Decoupling-based Defense (DBD) and Adaptive Splitting-based Defense (ASD). The semi-supervised learning parameters align with ASD, including 1024 training iterations, a temperature of 0.5, a ramp-up length of 120, and a learning rate of 0.002. The altruistic model undergoes a warm-up phase with 25 epochs, utilizing the Adam optimizer, Cross Entropy loss, with a learning rate of 0.001. The default warm-up epochs for the main model in OSS are set to 20 (followed by a 10-epoch training on the initialized pools)($T_1 = 20$), with a default β of 0.2. Class completion training spans 60 epochs ($T_2 = 90$), and selective dropping training spans 30 epochs ($T_3 = 120$). The altruistic model update uses the same loss and optimizer as in the warm-up on CIFAR-10 and Imagenet for efficiency, on lightweight datasets like GTSRB, we use the same semi-supervised loss and optimizer as the main model for better performance. The clean pool ratio α follows a sinusoidal growth curve during class completion training, starts at β, and reaches an upper limit of $\alpha = 0.6$ at the end of the class completion stage, after which it remains fixed:

$$\begin{aligned} T' &= \frac{T - T_1 - 10}{T_2 - T_1 - 10} T_2 \\ \alpha_T &= \beta + (\alpha - \beta) \times (1 - \cos(\pi \times T'/T_2))/2 \end{aligned} \tag{11}$$

The baselines are implemented using:

- BackdoorBench (Wu et al., 2022);
- BackdoorBox (Li et al., 2023b);
- Github repositories of corresponding papers.

We greatly appreciate these outstanding works.

C.5 Definition of DER

Defense Effectiveness Rating (DER) (Zhu et al., 2023a) is a comprehensive measure that considers both ACC and ASR:

$$\mathrm{DER} = [\max(0, \Delta\mathrm{ASR}) - \max(0, \Delta\mathrm{ACC}) + 1]/2, \tag{12}$$

where $\Delta\mathrm{ASR}$ denotes the decrease of ASR after applying defense, and $\Delta\mathrm{ACC}$ denotes the drop in ACC following the defense. Higher ACC, lower ASR and higher DER indicate better defense performance.

C.6 Details about semi-supervised loss

Semi-supervised learning (Berthelot et al., 2019a;b; Sohn et al., 2020; Xie et al., 2020; Zhu & Goldberg, 2022) studies how to leverage a training dataset with both labeled data and unlabeled data to obtain a model with high accuracy. In addition to its application in normal training, semi-supervised learning also serves as a powerful means for the security of DNNs (Alayrac et al., 2019; Carmon et al., 2019; Huang et al., 2022).

Here we adopt the MixMatch (Berthelot et al., 2019b). Given a batch $\mathcal{X} \subset \mathcal{D}_C$ of labeled samples, and a batch $\mathcal{U} \subset \mathcal{D}_P$ of unlabeled samples, MixMatch generates a guessed label distribution $\tilde{q}$ for each unlabeled sample $u \in \mathcal{U}$ and adopts MixUp to augment $\mathcal{X}$ and $\mathcal{U}$ to $\mathbf{X}\prime$ and $\mathbf{U}\prime$. The supervised loss $\mathcal{L}_s$ is defined as:

$$\mathcal{L}_s = \sum_{(x,q) \in \mathcal{X}'} \mathrm{H}\left(p_x, q\right), \tag{13}$$

where p_x is the prediction of x, q is the one-hot label and $H(\cdot,\cdot)$ is the cross-entropy loss. The unsupervised loss $\mathcal{L}_u$ is defined as:

$$\mathcal{L}_u = \sum_{(u,\bar{q})\in\mathcal{U}'} \|p_u - \bar{q}\|_2^2 \,, \tag{14}$$

where p_u is the prediction of u.

Finally, the MixMatch loss can be defined as:

$$\mathcal{L} = \mathcal{L}_s + \lambda \cdot \mathcal{L}_u, \tag{15}$$

where λ is a hyper-parameter for trade-off, we adopt the same $\lambda = 15$ as in ASD.

D Supplementary Information of the Background

D.1 Supplementary Overview of Backdoor Attack Research

The common implementation of backdoor attacks is realized by injecting a few poisoned samples into the training dataset, i.e., data-poisoning-based backdoor attacks, inducing the model to build a link between the trigger (i.e., a visual particular pattern) and target class (Gu et al., 2017). Thus the model consistently outputs the target label once the trigger is attached to the inputs in the inference stage.

Poison-label backdoor attacks are currently the most common attack paradigm, where the trigger pattern in the poisoned samples is directly connected to the target class by relabeling, inducing the model to treat the trigger as a decision-making feature of the target class. Recent research (Hu et al., 2022; Li et al., 2020; Qi et al., 2021) focuses on more invisible trigger designs through generative models and feature space optimizations, as well as exploring backdoor attacks in wider tasks like natural language processing.

D.2 Illustration of the Model Collapse

As presented in Figure 8, the splitting-based defenses (loss-guided ones specifically) encounter two kinds of model collapse. In backdoor overfitting collapse, poison samples take effect and have low loss values, which consistently corrupt the clean pool and lead to a backdoored model. Likewise, in class underfitting collapse, the rareness of certain classes will lead to higher loss values, making them less chosen to be clean samples, which forms a vicious cycle. Note that these two collapses are common in other categories of defenses as well, while it's more explainable in splitting-based defense.

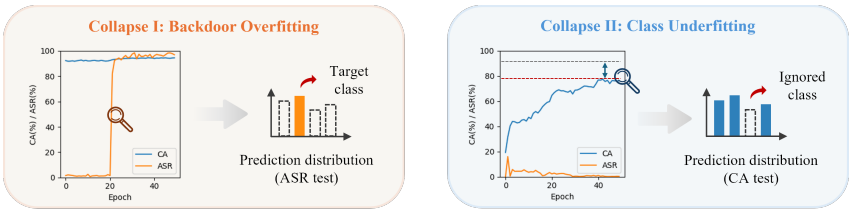

Figure 8: Typical model collapses in data-splitting backdoor defenses. **I**: Misclassification of low-loss poisoned samples as clean leads to a steady increase in the poisoned sample proportion until 100% ASR. **II**: Higher losses for challenging classes reduce their presence in the clean pool, rendering the model unable to predict samples from those categories.

E More Experimental Results

E.1 Illustration of Pool Update

To showcase the healthy clean pool acquired by our BSD, we plot the number of poison samples in the clean pool at each training epoch, as well as reveal the accumulated number of poison samples.

As shown in Figure 9, our BSD generally have fewer poison samples in the clean pool during training, with both the number of poisoned samples and the cumulative number of samples smaller than that fo ASD under different poisoning rates.

In addition, we plot the loss/distance distribution of samples of our BSD in Figure 10. In Figure 10.(a) and Figure 10.(b), the main mechanisms, i.e., ALS and OSS for the pool initialization, successfully distinguished the poison samples. In Figure 10.(c), the poison samples are highlighted by the high loss discrepancy between the main model and the altruistic model. The final result shown in Figure 10.(d) reveals the high CAs (clean sample all having low loss values) and low ASRs (poison samples all having high loss values) of BSD.

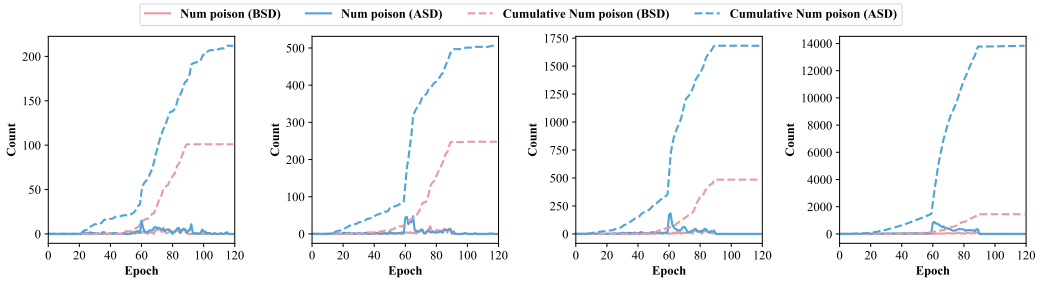

Figure 9: The number of poison samples in the clean pool of BSD and ASD at each epoch, the accumulated number in the dotted line. The subplots are the results on CIFAR-10, $\rho = 0.01, 0.05, 0.10, 0.20$.

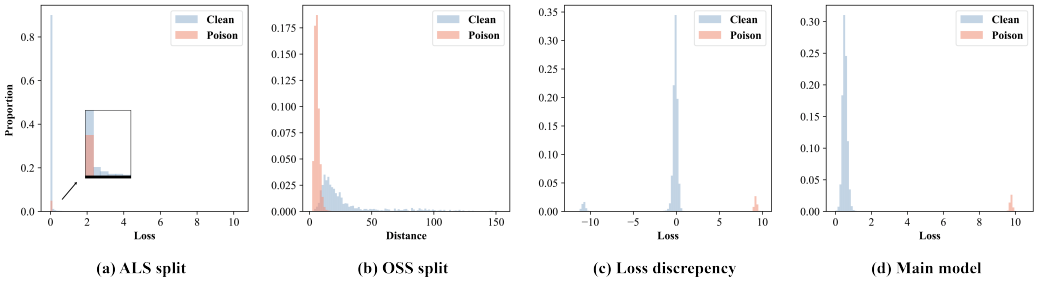

(a) ALS split (b) OSS split (c) Loss discrepency (d) Main model

Figure 10: The split visualization of BSD on GTSRB against the BadNet attack. (a) the loss distribution on the altruistic model after the ALS warm-up; (b) the distance distribution on the main model after the OSS warm-up; (c) the loss discrepancy at the last epoch; (d) the loss distribution on the main model at the last epoch.

E.2 Influence of different settings in OSS

Ablation on distance metric of OSS. We investigate the influence of the number of runs for the warm-up and three different distance calculations of OSS as shown in Figure 11. For the distance calculation, we take three approaches, i.e., the minimal, the maximal, and the mean ℓ_2 distance to feature clusters of each non-target category. Intuitively, we set the minimal distance by default, because the poisoned samples we consider are characterized by being far away from all existing cluster centers, thus maximal and mean distances may misjudgment two categories whose original clustering centers are far apart from each other as poisoned samples. Whereas, all three approaches exhibit good separation under the default 20-epoch warm-up.

Ablation on warm-up epochs of OSS (T_1). Concerning the number of warm-up epochs, we investigate the score distribution of OSS under the min-distance calculation. As illustrated in Figure 11, the result exhibits poor separation with an insufficient warm-up. As the number of epochs goes up, it has a certain effect when the number of epochs equals 10, and perfectly separates some benign samples with larger epochs.

Figure 11 is the complete result of the ablation study on different settings of the warm-up process of OSS. It verifies the effectiveness of all three distance metrics. Intuitively, the model should have a more separable and reliable initialization of the two pools with a long warm-up, whereas the result of a 40-epoch warm-up (especially when using the mean distance) violates this intuition by exhibiting less satisfying separation. A potential reason is that the model overfitted the non-target classes, thus the poison samples have less similarity to them.

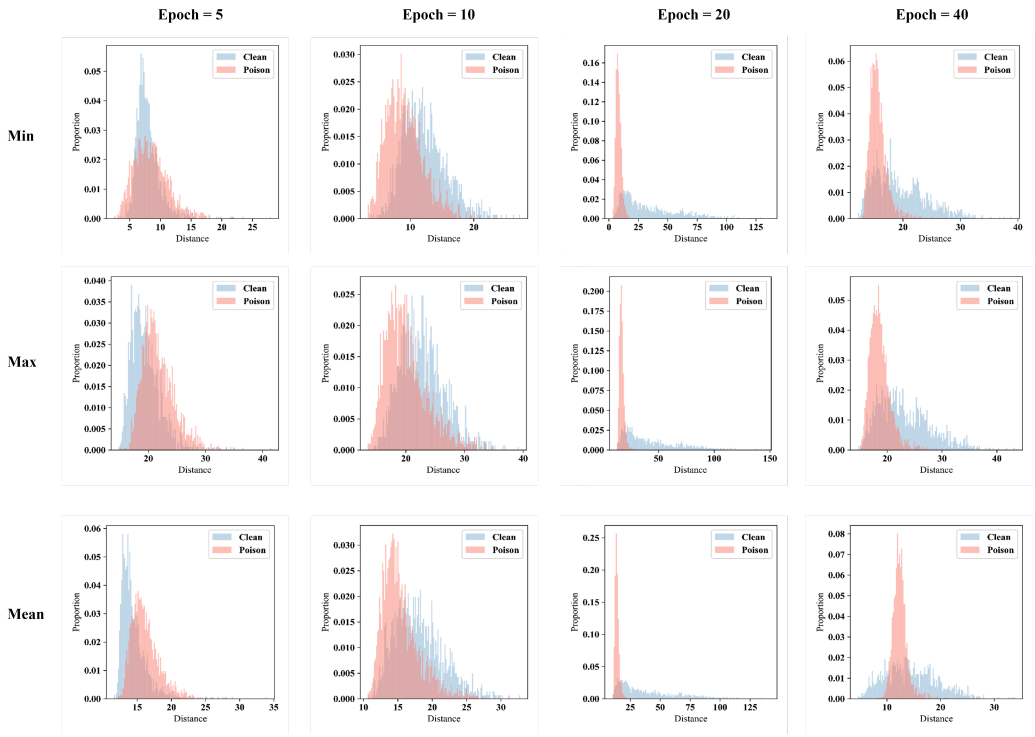

Figure 11: The ablation results on the number of warm-up epochs and different distance calculation methods for OSS.

In general, the default setting of BSD is a suitable choice.

E.3 Influence of different settings in ALS

Ablation study on warm-up epochs of the altruistic model. The warm-up of the altruistic model will determine the correctness of y_t. Instead of directly assuming y_t being known to the defender, we explored lightweight methods to approximate it. Zhu et al. (2024) uses the most frequent second likely prediction as approximated y_t, Gao et al. (2024) uses a likewise energy score, which is also effective. Li et al. (2021a) proposes to isolate the poison samples through a local gradient ascent process. If the detection precision exceeds 50%, it indicates that more than half of the isolated samples are poison samples, thus we can obtain y_t. Although the experimental results presented by Li et al. (2021a) in their Figure 7, page 16 has already verified a more than 50% against most common attacks, we further check its robustness to the warm-up epochs in Table 13.

Alternative method for approximating y_t For unseen failures that the local gradient ascent (Li et al., 2021a) can not correctly approximate y_t, we provide an alternative method for approximating y_t against new backdoor attacks that may appear in the future. Here we follow Zhu et al. (2024) to use the most frequent second likely prediction, i.e., $y_t = \text{argsort(-logit)[1]}$, where logit means the logit output of a DNN. However, this prediction could be unstable, we further statistics the predicted y_t in each warm-up epoch and use the majority as the final prediction of y_t. The effectiveness of the

Table 13: The prediction of y_t under different warm-up epochs. The 'num' represents the number of poison samples in the isolated set.

WARM-UP EPOCHS	BADNET		BLENDED	
	NUM POISON	y_t	NUM POISON	y_t
5	0	WRONG	0	WRONG
15	461	CORRECT	457	CORRECT
25	370	CORRECT	344	CORRECT
35	85	CORRECT	126	WRONG
45	177	CORRECT	114	CORRECT

alternative method is shown in Figure 12, where all the final majority predictions of y_t are the same ($y_t = 3$), which is the ground truth target label.

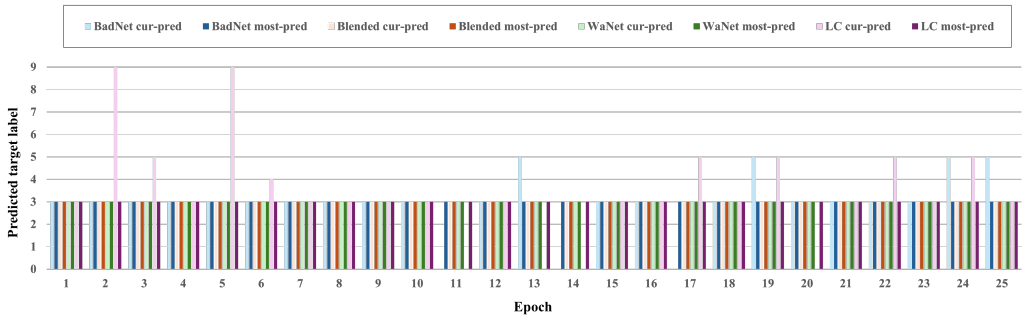

Figure 12: The result of the alternative method for y_t approximation. In the default 25 epochs of warm-up, we count the pred y_t at each epoch and the most pred y_t by that epoch respectively. The experiment is conducted on CIFAR-10, against BadNet, Blended, WaNat, and LC.

E.4 PERFORMANCE UNDER NO ATTACKS

Most backdoor defense research focuses on performance under attack, while it is concerning that these defenses may degrade model performance in the absence of attacks. Therefore, we evaluated the performance of BSD in scenarios without attacks. There are no poisoned samples in the training set, we test the clean and poisoned samples (BadNets trigger) for inference. As shown in Table 14, it is worth noting that even in the absence of attacks, there can be a low attack success rate (ASR), where these samples are just being misclassified to the target label. As Table 14 reveals, our method achieves a lower ASR compared to the baseline, effectively suppressing natural backdoors. Additionally, our method shows significant improvements in accuracy over the baseline.

Table 14: The clean accuracy (CA%) and attack success rate (ASR%) of BSD and ASD under no attacks.

METHOD	CIFAR-10		GTSRB	
	ACC	ASR	ACC	ASR
NO DEFENSE	95.3	1.9	97.7	0.2
ASD	93.2	1.8	96.6	0.1
BSD (OURS)	94.9	0.6	97.6	0.0

E.5 RESISTANCE TO POTENTIAL ADAPTIVE ATTACKS

In the above experiments, we assume that attackers have no information about our backdoor defense. In this section, we consider a more challenging setting, where the attackers know the existence of our defense and can construct the poisoned dataset with an adaptive attack.

Threat model for the attackers. Following existing work (Gao et al., 2023; Chen et al., 2017; Gu et al., 2017; Turner et al., 2018), we assume that the attackers can access the entire dataset and know

the architecture of the victim model. However, the attackers can not control the training process after poisoned samples are injected into the training dataset.

Method for adaptive attack. Our method initializes the clean pool using bi-perspective splitting through OSS and ALS, which separate poisoned samples based on semantic and loss statistics, respectively. In general, there is a contradiction between increasing the loss values of poisoned samples (to bypass ALS) and achieving backdoor objectives. Furthermore, maintaining high semantic similarity to the target class (to bypass OSS) adds to the complexity. To craft such a trigger pattern that satisfies the above objectives, we use a PGD optimization to search for an average noise (among non-target classes) that is semantically close (judged by a proxy model) to the target class (to bypass OSS). Meanwhile, we control the ℓ_∞ ball bound as 8/255 and the poisoning rate as 0.01 to prevent it from being an obvious trigger that will be easily fitted (to bypass ALS).

Settings. We conduct experiments on CIFAR-10 with the following parameters: number of iterations, 15; step size, 1.5/255; perturbation magnitude, 8/255; trigger size, 32×32; and poisoning rate, 0.01. Although the attacker is assumed to have no knowledge of the model structure, we adopt a more challenging setting where the adversary uses the same model structure as the proxy model.

Results. The Clean Accuracy (CA) and Attack Success Rate (ASR) of this adaptive attack are 94.422% and 2.421%, respectively. While the ASR is slightly higher than that of other attacks on CIFAR-10, our defense clearly demonstrates strong resistance to the adaptive attack. Furthermore, when we increase the poisoning rate to 0.2 (20%), the CA and ASR remain at 91.040% and 0.903%, respectively, which is still within an acceptable range.

E.6 Searching the best result of baselines

Notably, some baseline methods are sensitive to their hyper-parameter settings. The results reported in Table 1 represent their best performance obtained through grid search, as outlined in ASD (Gao et al., 2023). Similarly, for the additional attack settings, the results in Table 2 and Table 3 are based on their best outcomes (ranking on DERs) after grid search. For DBD, which is not sensitive to parameters, we report the best result using the default settings from BackdoorBench and the same configuration as in ASD.

Table 15: Grid search for FP against additional attacks on ResNet18 (Default represents the result under the default setting provided by backdoorbench).

Ratio	LC		SIG		Refool		Narcissus	
	CA	ASR	CA	ASR	CA	ASR	CA	ASR
Default	87.1	24.4	87.1	60.8	86.5	23.0	87.2	63.4
0.1	87.3	79.8	87.2	81.4	86.8	25.6	87.4	72.4
0.2	87.0	59.4	87.0	82.4	86.5	28.0	86.7	77.8
0.3	86.7	51.6	87.0	83.2	86.5	27.6	87.2	73.9
0.4	87.0	49.0	87.2	85.7	86.4	28.8	87.2	77.6
0.5	85.7	67.3	86.2	86.1	85.2	29.6	86.7	79.0
0.6	86.0	73.6	86.7	90.1	85.6	31.6	86.6	80.7
0.7	86.3	80.0	86.8	88.5	86.1	31.0	87.1	79.6
0.8	87.0	74.9	86.9	87.7	86.4	28.3	87.3	78.5
0.9	87.3	62.0	87.0	80.3	86.5	25.2	87.6	72.3

Table 16: Grid search for FP against representative attacks on Mobilenetv2 (Default represents the result under the default setting provided by backdoorbench).

Ratio	BadNet		Blended		WaNet	
	CA	ASR	CA	ASR	CA	ASR
Default	77.9	8.3	75.9	30.8	82.2	2.4
0.1	80.8	58.3	78.4	57.9	79.3	3.0
0.2	79.6	84.0	78.6	56.1	80.1	3.8
0.3	80.6	99.8	79.0	51.8	77.2	5.8
0.4	79.5	73.5	77.8	53.7	77.3	4.4
0.5	79.5	10.9	77.1	70.0	78.3	1.3
0.6	79.7	19.3	76.6	67.3	78.6	2.0
0.7	79.1	61.7	76.3	65.7	79.1	1.9
0.8	79.7	12.7	77.3	66.1	78.3	1.2
0.9	80.4	99.2	78.4	62.6	79.3	2.5

Table 17: Grid search for NAD against additional attacks on ResNet18 (Default represents the result under the default setting provided by backdoorbench).

Beta	LC		SIG		Refool		Narcissus	
	CA	ASR	CA	ASR	CA	ASR	CA	ASR
Default	86.2	69.7	86.0	83.6	85.3	49.3	86.1	84.9
100	87.3	98.7	87.1	95.9	86.5	66.9	86.8	93.3
500	86.2	69.7	86.0	83.6	85.3	49.3	86.1	84.9
1000	86.2	69.7	86.0	83.6	85.3	49.3	86.1	84.9
1500	86.2	69.7	86.0	83.6	85.3	49.3	86.1	84.9
2000	86.2	69.7	86.0	83.6	85.3	49.3	86.1	84.9
2500	86.2	69.7	86.0	83.6	85.3	49.3	86.1	84.9
5000	86.2	69.7	86.0	83.6	85.3	49.3	86.1	84.9
7500	86.2	69.7	86.0	83.6	85.3	49.3	86.1	84.9
1.E+04	86.2	69.7	86.0	83.6	85.3	49.3	86.1	84.9
1.E+05	86.2	69.7	86.0	83.6	85.3	49.3	86.1	84.9
1.E+06	86.2	69.9	85.8	83.3	85.3	49.3	86.2	84.9
1.E+07	85.9	50.5	85.7	84.5	85.5	46.5	86.5	81.0
1.E+08	86.0	73.9	85.8	88.7	85.6	42.9	86.1	83.2
1.E+09	85.3	68.2	85.7	87.0	85.6	44.8	86.5	84.1
1.E+10	85.9	69.5	85.8	83.0	85.4	47.7	86.0	86.2
1.E+11	85.9	65.6	85.7	86.3	85.6	42.5	86.4	83.4

Table 18: Grid search for NAD against representative attacks on Mobilenetv2 (Default represents the result under the default setting provided by backdoorbench).

Beta	BadNet		Blended		WaNet	
	CA	ASR	CA	ASR	CA	ASR
Default	78.5	11.7	76.2	51.6	81.1	4.2
100	79.7	99.1	79.5	56.8	77.3	3.4
500	78.5	11.7	76.2	51.6	81.1	4.2
1000	78.5	11.7	76.2	51.6	81.1	4.2
1500	78.5	11.7	76.2	51.6	81.1	4.2
2000	78.5	11.7	76.2	51.6	81.1	4.1
2500	78.5	11.7	76.2	51.6	81.1	4.1
5000	78.5	11.7	76.2	51.6	81.1	4.1
7500	78.5	11.7	76.2	51.6	81.1	4.1
1.E+04	78.5	11.7	76.2	51.6	81.1	4.1
1.E+05	78.6	29.1	76.1	51.3	79.8	4.0
1.E+06	78.5	23.0	75.9	49.4	81.5	3.2
1.E+07	79.3	25.4	76.8	47.6	81.0	3.8
1.E+08	78.8	14.8	76.8	58.9	81.0	3.2
1.E+09	78.9	17.9	76.0	46.0	80.7	5.4
1.E+10	79.2	25.0	76.5	51.8	81.6	4.1
1.E+11	78.8	41.5	76.7	56.9	81.3	4.3

Table 19: Grid search for ABL against additional attacks on ResNet18 (Default represents the result under the default setting provided by backdoorbench).

Gamma	LC		SIG		Refool		Narcissus	
	CA	ASR	CA	ASR	CA	ASR	CA	ASR
Default	71.1	4.3	37.5	0.0	63.3	94.0	62.7	0.4
0.0	81.2	7.3	81.2	74.6	79.4	86.4	80.7	76.7
0.1	81.2	6.0	79.7	41.5	72.0	93.5	80.3	35.1
0.2	80.3	3.8	73.9	16.5	76.3	82.0	79.4	32.7
0.3	78.1	0.9	76.1	14.4	76.0	86.5	79.3	7.1
0.4	80.2	1.6	67.6	5.1	71.4	85.4	76.6	44.1
0.5	78.7	1.0	67.0	6.9	75.2	93.8	78.3	17.5

Table 20: Grid search for ABL against representative attacks on Mobilenetv2 (Default represents the result under the default setting provided by backdoorbench).

Gamma	BadNet		Blended		WaNet	
	CA	ASR	CA	ASR	CA	ASR
Default	68.0	24.4	67.3	2.6	50.9	0.5
0.0	81.3	36.9	77.3	21.6	68.9	74.8
0.1	81.3	36.9	77.3	21.6	68.9	74.8
0.2	81.3	36.9	77.3	21.6	68.9	74.8
0.3	81.3	36.9	77.3	21.6	68.9	74.8
0.4	79.7	13.6	78.4	15.1	68.9	74.8
0.5	81.3	48.1	80.4	33.4	68.9	74.8

Table 21: Result of DBD against additional attacks on ResNet18 (Default represents the result under the default setting provided by backdoorbench, Default2 represents the recommended setting used in ASD).

Setting	LC		SIG		Refool		Narcissus	
	CA	ASR	CA	ASR	CA	ASR	CA	ASR
Default	83.2	98.1	77.6	99.9	87.0	0.1	87.3	99.6
Default2	82.46	99.42	80.12	99.9	90.84	2.34	80.73	99.61

Table 22: Result of DBD against representative attacks on Mobilenetv2 (Default represents the result under the default setting provided by backdoorbench, Default2 represents the recommended setting used in ASD).

Setting	BadNet		Blended		WaNet	
	CA	ASR	CA	ASR	CA	ASR
Default	65.5	0.0	69.0	0.0	58.4	12.4
Default2	54.34	0	64.22	0	57.22	14.11